The Pennsylvania State University

The Graduate School

Energy and Mineral Engineering

PREDICTION OF BOUNDARY-DOMINATED FLOW FOR LOW PERMEABILITY RESERVOIRS USING EARLY-TRANSIENT DATA

A Thesis in

Energy and Mineral Engineering

by

Yuzhe Cai

Submitted in Partial Fulfillment
of the Requirements
for the Degree of

Master of Science

August 2017

The thesis of Yuzhe Cai was reviewed and approved* by the following:

Luis F. Ayala H.
William A. Fustos Family Professor
Professor of Petroleum and Natural Gas Engineering;
Associate Department Head for Graduate Education

Shimin Liu
Assistant Professor of Energy and Mineral Engineering

Eugene Morgan
Assistant Professor of Petroleum and Natural Gas Engineering

Sanjay Srinivasan
Professor of Petroleum and Natural Gas Engineering;
John and Willie Leone Family Chair in Energy and Mineral Engineering
Interim Associate Department Head for Graduate Education

*Signatures are on file in the Graduate School

ABSTRACT

Unconventional natural gas resources have become an important energy supply in North America. Shale gas and tight gas provides over half of the natural gas production in the United States. Linear flow is the most common flow type in tight and shale gas reservoirs. A density-based analytical approach was proposed by Vardcharragosad and Ayala (2014) that could predict well production performance in the linear flow regime. However, this approach requires reservoir and fluid properties for the prediction. As matter of fact, most of these reservoir properties are unknown and undetermined. The thrust of this study is to predict the long-term (Boundary-dominated period) well production behavior with the reservoir properties as inputs through an updated density-based approach.

The BDF model proposed in this study is based on Vardcharragosad and Ayala's density-based approach (2015). A novel and key task for the BDF production prediction is the utilization of historical production data, which is often termed as Production Data Analysis (PDA). A PDA technique is used to estimate the characterization ratio, which is applied to replace reservoir properties in the prediction model. In addition, transition time needs to be determined to estimate reservoir size because it determines the starting point of the boundary-dominated flow. By using the estimated characterization ratio and the transition time, the novel density-based approach could be re-constructed without inputting specific reservoir properties. The proposed model was initially validated with numerical simulation results.

This thesis presents a method to predict boundary-dominated flow behavior in tight and shale gas reservoirs without the knowledge of reservoir properties. The proposed transition time determination approach shows advantages over traditional

end of half slope method. Thus, original gas in place can be directly calculated from results of transition time determination and early data analysis more accurately. Also, cost of techniques on determining reservoir properties such as well logging could be reduced.

Table of Contents

LIST OF FIGURES

LIST OF TABLES

ACKNOWLEDGEMENTS

First of all, I want to express my sincere gratitude to both of my advisors – Dr. Luis F. Ayala and Dr. Shimin Liu, who gave me continuous help and encouragement throughout my master study. They are always helpful and patient. Without their help, I could not have finished my work.

I also want to express my thanks to my committee member – Dr. Eugene Morgan for his precious time and suggestions to improve this work.

I want to give my thanks to my friends in Penn State. They are always around and giving me encouragement. I want to give my special thanks to my parents who always give me very valuable love and support at any time.

NOMENCLATURE

A	reservoir area, L^2, ft^2
A_r	reservoir area inside ROI, L^2, ft^2
B_{gi}	gas formation volume factor at initial conditions, RB/scf
B_o	oil formation volume factor, RB/STB
c_g	gas compressibility, L-t^2/M, psi^{-1}
c_t	total compressibility, L-t^2/M, psi^{-1}
C_r	coefficient used to calculate radius of influence, dimensionless
CGIP	contact gas in place, scf
D	decline rate, 1/t, 1/day
G_p	cumulative gas production, L^3, SCF
h	reservoir thickness, L, ft
k	permeability, L^2, md
OGIP	original gas in place, scf
m(p)	gas pseudo-pressure, psia^2/cp
MW	molecular weight, lb/lbmol
P	pressure, psia
Pi	initial reservoir pressure, psia
P_{wf}	well bottom-hole pressure, psia
q_D	dimensionless flow rate
MW	molecular weight, M/mole, 1b/1bmol
n_r	exponent used to calculate radius of influence, dimensionless
p	pressure M/L-t^2,psia
q_{gsc}	gas flow rate, L^3/t, scfd

q_D	dimensionless flow rate
q_{Dd}	decline dimensionless flow rate
r	radius/distance from wellbore, L, ft
r_e	external (outer reservoir) radius, L, ft
r_{inf}	radius of influence, L, ft
r_w	wellbore (inner reservoir) radius, L, ft
r_ρ	wellbore-to-initial density ratio, dimensionless
R	universal gas constant, M-L^2/t^2-T-mole, 10.73 ft^3-psi/R-1bmol
t	time, days
t_D	dimensionless time
t_{DAD}	decline dimensionless time
T	reservoir temperature, F
T_{sc}	temperature at standard condition, F
s	Laplace variable
x_f	half fracture length, ft
Z	gas compressibility factor
μ_g	gas viscosity, cp
μ_{gi}	gas viscosity at initial condition, cp
ϕ	porosity, fraction
ϕ_{i}	porosity at initial reservoir pressure, fraction
ρ	gas density, lbm/ft^3
ρ_i	gas density at initial reservoir pressure, lbm/ft^3
$\bar{\rho}$	gas density at average reservoir pressure, lbm/ft^3
ρ_{sc}	gas density at standard condition, lbm/ft^3
ρ_{wf}	gas density at standard condition, lbm/ft^3

$\bar{\lambda}$ average viscosity-compressibility dimensionless ratio between initial reservoir pressure and average reservoir pressure

$\bar{\beta}$ the time-averaged value of $\bar{\lambda}$

α_1 unit conversion constant, 6.328*10-3 (ft^2-cp) / (psi-md-day)

CHAPTER 1 - INTRODUCTION

Tight gas and shale gas resources have been receiving much attention in recent years. As conventional gas resources are declining, tight gas and shale gas have become increasingly important components of natural gas production in the United States. According to EIA 2016, these two components are responsible for approximately 70% of US dry natural gas production; the fraction is expected to reach 85% in 2040 (see Figure 1-1). Both are classified as unconventional natural gas resources because of their extremely low permeability and unique extraction technologies. Therefore, they could not be produced economically without effective reservoir stimulations. Routinely, horizontal drilling and hydraulic fracturing are used to achieve economically flowrates.

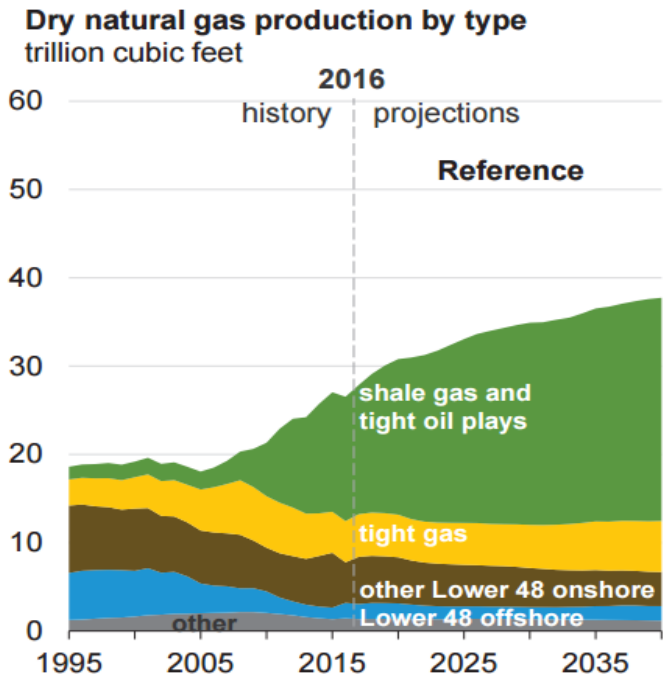

Figure 1-1 U.S. dry natural gas production by source in the Reference case, 1995–2040， trillion cubic feet (EIA 2017)

Linear flow is a typical flow regime occurring in hydraulically-fractured unconventional gas plays. Due to extremely low permeability of the formations, hydraulic fractures are needed to gain economic flowrate in these reservoirs. It has been observed that many tight and shale gas wells could produce in linear flow regime for over 10 or 20 years characterized by factures with infinite conductivity and extend nearly to or to both ends of each reservoir (Graphical representation of linear flow system see Figure 2-1 (Watternbarger et al., 1998)).

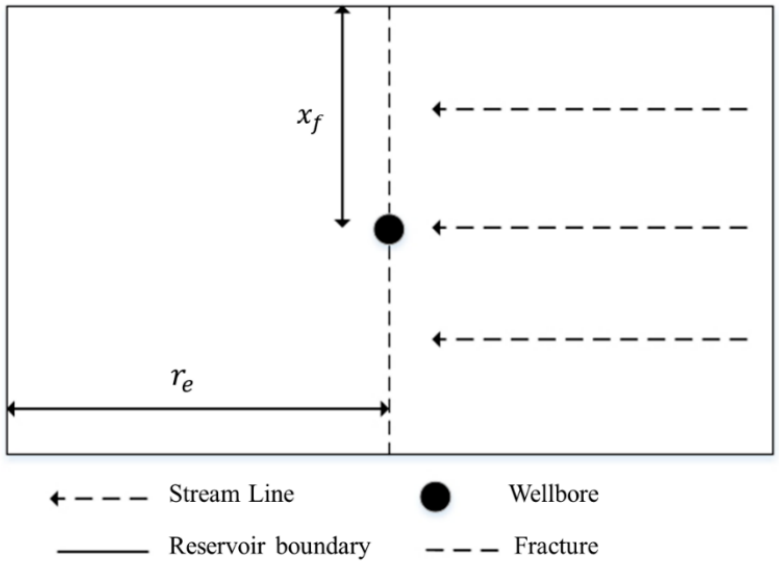

Figure 1-2 Graphical representation of linear flow system (Top View)

Therefore, linear flow characterization and quantification are crucial for understanding, analyzing and predicting well production performance in these low permeability tight gas reservoirs. Ye and Ayala (2012) proposed a density-based approach to analyze radial flow within gas reservoirs. In this density-based approach the gas diffusivity equation is solved by using a density-based transformation. By using two depletion driven dimensionless variables - λ and β, this density-based method is able to model the performance of gas wells by rescaling available liquid

solutions. Vardcharragosad (2014) extended the density-based method to shale and tight gas reservoirs. The preceding Boundary-Dominated Flow (BDF) models proposed by Vardcharragosad (2014) could predict the well production in shale and tight gas reservoirs if precise values of reservoir and fluid properties are available. However, in most situations, reservoir engineers and modelers do not have prior knowledge of these reservoirs. Hence, the use of early data, is of great importance to obtain important insight about reservoir properties. The objective of this study is to arrive at an analytical method to predict BDF performance in unconventional shale and tight gas reservoirs without prior knowledge of reservoir properties. With the proposed method, original gas in place could be estimated as well. This proposed method could help save a large amount of cost on techniques of determining reservoir properties. To achieve this objective, it is proposed to use only production data related to early transient flow and an accurate time when BDF starts to evaluate and predict the production performance of an unconventional gas well.

In this thesis, Chapter 1, as provided above, presents an introduction and background information to the research topic. Chapter 2 shows previous studies with regards to the research topic. Chapter 3 presents all the methodologies developed in this study, which includes two approaches to determine transition time, an early time PDA approach and BDF prediction models. In Chapter 4, 64 numerical cases studies are presented to validate the proposed models. Also, two field cases are presented to further test the applicability of the models. In the last section, conclusions of the study is presented.

CHAPTER 2 - BACKGROUND AND LITERATURE REVIEW

Generally, oil/gas flows in reservoirs can be divided into early transient flow and boundary-dominated flow (BDF). During the early transient period, fluid migrates from an increasing drainage area into the wellbore, before fluid depletion reaches the reservoir's boundary. In the boundary-dominated period, the entire reservoir depletes at the same time as fluid depletion has reached the boundary. This process is illustrated in Figure 2-1. During an early transient period, pressure decline hasn't reached the boundary whereas, pressure declines simultaneously across the entire reservoir during the boundary-dominated period. With the aid of production data analysis at the early transient period, this study seeks to predict boundary-dominated flow behavior in unconventional tight and shale gas reservoirs without the direct inputs of reservoir properties.

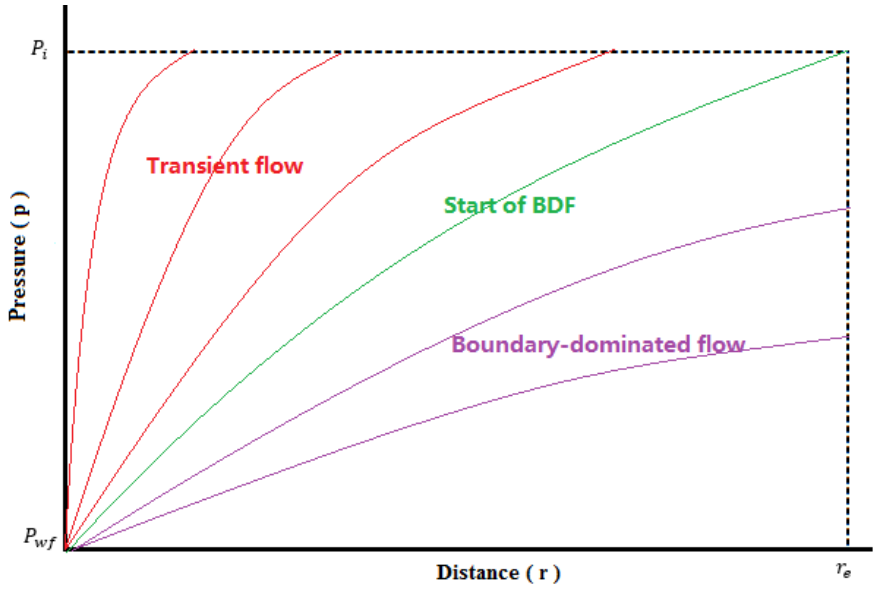

Figure 2-1 Graphic Representation of Early Transient Flow and Boundary Dominated Flow

Due to the extremely low permeability of unconventional tight and shale gas reservoirs, the reservoir formation has to be hydraulically fractured to ensure the flow

deliverability and thus economic gas flowrates. When the fracture extends to (or nearly to) both ends of the reservoir boundary, linear flow can be expected to dominate the flow regime. Although hydraulic fractures are created to enhance the production rate, the extremely low matrix permeability still leads to a long period of early transient flow. It is important to use a production data analysis technique to early transient flow data to define the flow regimes and arrive the inputs for the BDF prediction. This study focuses on the case of constant bottomhole pressure condition.

When other reservoir properties are known, the application of the traditional production data analysis method of linear flow into low permeability reservoirs enables the extraction of the $x_f\sqrt{k}$ values (Wattenbarger et al. (1998)). The thrust of this study is the prediction of long-term well performance without detailed knowledge of reservoir properties. New production data analysis techniques are presented in this study and, by the aid of these techniques, BDF performance was predicted without the luxury of knowledge of many reservoir properties.

This chapter firstly presents a review of gas solutions for infinite-acting reservoirs under the constant P_{wf} specification. This is then followed by an introduction to Region of Influence (ROI), an important concept enabling early transient solution. Following this, a review of certain production data analysis techniques developed from early transient gas solution and transition time determination techniques is described. Finally, a review of BDF gas solution under constant P_{wf} production is presented. The proposed BDF prediction approach is an extension of the BDF model reported by Vardcharragosad (2014).

2.1 A review of gas solution during the early transient period - constant P_{wf}

Early transient flow refers to the period when fluid migrates from an increasing drainage area into the wellbore before fluid depletion reaches the reservoir boundary. The early transient flow behavior is of great importance to predict the BDF behavior.

Van Everdingen and Hurst (1949) have proposed a constant P_{wf} liquid solution for linear flow system as shown in Figure 2-2. In the Laplace domain, the solution utilizes a Laplace variable, s, defined as the following equation:

$$q_D = \frac{2}{\pi}\frac{1}{\sqrt{s}} \qquad \text{Equation 2-1}$$

This can be expressed in real time domain as (Wattenbarger et al., 1998):

$$q_D = \frac{2}{\pi}\frac{1}{\sqrt{\pi t_D}} \qquad \text{Equation 2-2}$$

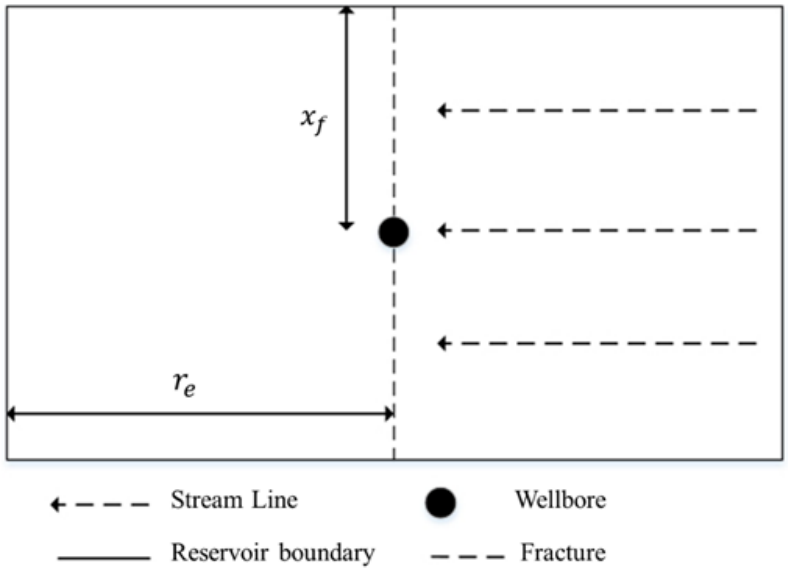

Figure 2-2 Graphical representation of a linear flow system (top view)

q_D and t_D are dimensionless flow rate and dimensionless time for oil, respectively and the definitions of the dimensionless variables are as follows:

$$q_D = \frac{q_{osc} B_o \mu_o}{\alpha_1 2\pi kh(P_i - P_{wf})} \quad \text{Equation 2-3}$$

$$t_D = \frac{\alpha_1 kt}{\phi \mu_o c_t {x_f}^2} \quad \text{Equation 2-4}$$

The oil rate calculations are nondimensionalized using B_o (oil formation volume factor), μ_o(oil viscosity), k (permeability), h (reservoir thickness), $P_i - P_{wf}$ (the difference between initial pressure and bottomhole pressure, ϕ (porosity), c_t (total compressibility) and x_f (half fracture length). α_1 is an unit conversion constant, which equals to 6.328*10-3 (ft^2-cp) / (psi-md-day). For gas systems, the diffusivity equation for linear flow is linearized by using pseudo-functions. The same liquid solution can be applied to the gas system if the pressure is expressed in terms of pseudo pressure, ψ (Al-Hussainy et al., 1966) and pseudo-time, t_a, (Agrawal 1979; Fraim and Wattenbarger, 1987). The dimensionless variables are defined as:

$$q_D = \frac{P_{sc}}{\alpha_1 \pi T_{sc}} \frac{q_{gsc} T}{kh(\psi_i - \psi_{wf)}} \quad \text{Equation 2-5}$$

$$t_D = \frac{\alpha_1 k t_a}{\phi \mu_{gi} c_{gi} {x_f}^2} \quad \text{Equation 2-6}$$

Pseudo variables for linear flow are defined as:

$$\psi = 2 \int_o^p \frac{p}{\mu_g Z} dp \quad \text{Equation 2-7}$$

$$t_a = \int_o^t \frac{\mu_{gi} c_{gi}}{\bar{\mu}_g \bar{c}_g} dt \qquad \text{Equation 2-8}$$

Based on observations of production data analysis from tight and shale gas reservoirs which exhibit linear flow behavior, Wattenbarger et al. (1998) suggested that t_D in Equation 2-4 could be defined in terms of actual time - *t* during the early transient period. The linear relationship between $1/q_{gsc}$ (gas flow rate) and $\sqrt{t}$ simplifies the production data analysis technique.

The classical gas solution during early transient period under a constant bottomhole pressure is based on application of pseudo pressure. A density-based approach was originally proposed by Ye and Ayala (2012), which could model BDF behavior without employing pseudo-functions. This approach can obtain gas solutions for radial flow under a constant bottomhole pressure by implementing a $\bar{\lambda} - \bar{\beta}$ rescaling as follows:

$$q_D^{gas}(t_D) = \bar{\lambda} \cdot q_D^{liq}(\bar{\beta} t_D) \qquad \text{Equation 2-9}$$

The viscosity/compressibility ratio $\bar{\lambda}$ between initial reservoir pressure and average reservoir pressure was derived originally by Ye and Ayala (2012), which has been improved rigorously by Ayala and Zhang (2013) as:

$$\bar{\lambda} = \frac{\mu_{gi} c_{gi}}{\bar{\mu}_g \bar{c}_g} = \frac{\mu_{gi} c_{gi}}{2\theta(\frac{\bar{\rho} - \rho_{wf}}{\bar{\psi} - \psi_{wf}})} \qquad \text{Equation 2-10}$$

$\bar{\mu}_g \bar{c}_g$ represents average fluid viscosity-compressibility between average reservoir condition and bottom-hole condition and $\theta = RT/MW$

$\bar{\beta}$ is defined as the time-averaged value of the viscosity/compressibility ratio:

$$\bar{\beta} = \frac{1}{t}\int_0^t \bar{\lambda}\, dt \qquad \text{Equation 2-11}$$

The dimensionless variables are defined in terms of density as:

$$q_D{}^* = \frac{q_{gsc}\mu_i c_i \rho_{sc}}{\alpha_1 2\pi kh(\rho_i - \rho_{wf)}} = Y \cdot \frac{q_{gsc}}{r_\rho} \qquad \text{Equation 2-12}$$

$$t_D{}^* = \frac{\alpha_1 kt}{\phi \mu_{gi} c_{gi} {x_f}^2} = X \cdot t \qquad \text{Equation 2-13}$$

$*$ denotes that the dimensionless variables are in the form of density.

Pressure dependent variables $\bar{\lambda}$ and $\bar{\beta}$ could be used to obtain gas responses by displacing liquid solutions. The definitions of $\bar{\lambda}$ and $\bar{\beta}$ shown in Equation 2-12 and Equation 2-13 are valid when $c_t = c_g$ (assuming rock compressibility = 0). It could be noticed that $\bar{\lambda}$ = $\bar{\beta}$ = 1 for liquid case and Equation 2-9 collapses to the original liquid solution. The original density-based transformation proposed by Ye and Ayala (2012) was developed for radial flow only. Vardcharragosad (2014) extended the density-based transformation to linear flow, which is often exhibited in shale gas and tight gas reservoirs. Vardcharragosad's work shows transformation equation in Equation 2-9 can be used for linear flow regime. Vardcharragosad's constant P_{wf} gas solution for early transient flow period is given as:

$$q_D = \sqrt{\bar{\lambda}}\,\frac{2}{\pi}\frac{1}{\sqrt{\pi t_D}} \qquad \text{Equation 2-14}$$

Originally, the average density calculated by material balance was based on the entire reservoir which introduces significant estimation errors. Anderson and Mattar (2007) suggested that the calculation of material balance statement could be based on region of influence (ROI) rather than the entire reservoir and the next section introduces the concept of ROI.

2.2 Concept of region of influence

Region of influence (ROI) is a very important concept proposed by Anderson and Mattar (2007). This technique significantly enhances the accuracy of production data analysis (PDA). In traditional PDA (Wattenbarger et al., 1998; Ibrahim and Wattenbarger, 2006), pseudo variables are calculated based on the average pressure across the entire reservoir, which results in estimation errors. Anderson and Mattar (2007) suggest that the calculation of average viscosity and compressibility should be based on the average pressure within the region of influence. The application of ROI enables linearization of the linear gas diffusivity equation because the average pressure within ROI has been proved to be constant during early transient period.

Anderson and Mattar (2007) firstly define ROI by introducing a radius of investigation, r_{inf}, defined as:

$$r_{inf} = C_r \cdot \left(\frac{\alpha_1 kt}{\phi \mu_{gi} c_{gi}}\right)^{0.5} + r_0 \qquad \text{Equation 2-15}$$

where, r_0 is the radius of the inner boundary ($r_0 = 0$ for linear flow and $r_0 = r_w$ for radial flow) and C_r is a controlling parameter which controls how fast the drainage

area increases. Anderson and Mattar (2007) adopted the classical C_r value of 2. Different C_r values ranging between 0.379 and 4.29 have been used under different conditions (Kuchuk, 2009). Nobakht and Clarkson (2012) found that using the classical value of 2 underestimates reservoir average pressure within ROI in comparison to the numerical simulation results. Therefore, they proposed a correction of calculation of reservoir average pressure using material balance statement based on numerical simulation, which is equivalent to using a C_r value of 2.554. I will use this value throughout this thesis.

The concept of ROI was based on that reservoirs of different sizes but with identical reservoir and fluid properties and produced under the same production specifications should have identical reservoir responses during the early transient period. A graphical representation is shown in Figure 2-3. At any time t during early transient period, reservoir A and reservoir B have identical average pressure within ROI (inside both yellow zones); but the average pressure within the entire reservoir will be different. Also, $\bar{\lambda}\ and\ \bar{\beta}$ estimations for linear early transient solution should be based on the average pressure within the ROI.

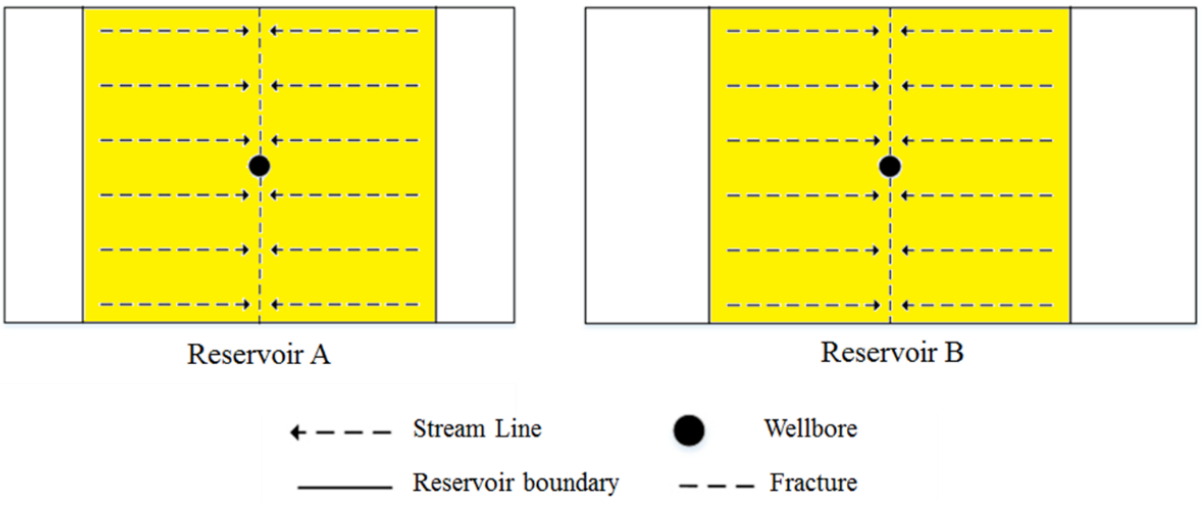

Figure 2-3 Graphical representation of the Region of Influence concept for linear flow

For dry gas reservoirs, Anderson and Mattar (2007) suggested using material balance equation to evaluate average pressure within ROI:

$$\frac{\bar{P}}{Z} = \frac{P_i}{Z_i}(1 - \frac{G_p}{CGIP}) \quad \text{Equation 2-16}$$

In the density form, the material balance equation can be expressed as:

$$\frac{\bar{\rho}}{\rho_i} = (1 - \frac{G_p}{CGIP}) \quad \text{Equation 2-17}$$

where CGIP represents the gas volume in place within ROI:

$$CGIP = \frac{A_r h \phi \rho_i}{\rho_{sc}} \quad \text{Equation 2-18}$$

where, A_r represents the reservoir area inside the ROI and r_{inf} stands for radius of investigation. For a linear flow system:

$$A_r = 4 x_f r_{inf} \quad \text{Equation 2-19}$$

Vardcharragosad (2014) defined Normalized Pressure Drawdown (NPD) as the normalized pressure difference between any reservoir location at any time:

$$NPD(r,t) = \frac{P(r,t) - P_{wf}}{P_i - P_{wf}} \quad \text{Equation 2-20}$$

By using the concept of radius of investigation, Vardcharragosad evaluated NPD for linear flow at the location $r = r_{inf}$:

$$NPD(C_r) = 1 - erfc(\frac{C_r}{2}) \quad \text{Equation 2-21}$$

From Equation 2-21, the NPD at the location $r = r_{inf}$ is a time-independent variable. According to C_r value of 2.554, NPD at the outer boundary of drainage area should always be found to be 7% using Equation 2-21. This pressure drawdown criterion will be used in a later section devoted to a transition time determination process called "Analogous filling-back procedure".

2.3 Review of production data analysis techniques

Production data analysis (PDA) is a useful tool for estimating reservoir reserves and forecasting well performance, which is very important in economic analysis of the field exploration and development. Arp's decline model (1945) is a classical PDA techniques. In Arp's model, the production decline can be classified into exponential decline, harmonic decline and hyperbolic decline based on a decline exponent (b). For a gas system, the decline parameters are determined through empirical curve fitting of historical production data. Fetkovich (1980) analytically proved that undersaturated oil production under volumetric depletion exhibits exponential decline (b = 0). Fetkovich et al. (1996) further showed that typical gas production exhibits hyperbolic decline with b = 0.40-0.50, and the b value is empirically determined. There are some well-known techniques that could accurately estimate OGIP based on production data during BDF period: the use of material balance pseudo-time (Palacio and Blasingame, 1993) and flowing material balance formulation (Mattar and Anderson, 2003). In this study, we focus on the production data analysis during early transient period.

For early transient period in a classical linear flow system, Wattenbarger et al. (1998) proposed a PDA approach for low permeability reservoirs producing in the early transient flow period under constant P_{wf} specification. The gas linear flow solution proposed by Wattenbarger indicates that, under a constant bottomhole pressure, a plot of $1/q$ vs. $\sqrt{t}$ is a straight line before the beginning of BDF. The slope of this straight line is used to calculate $x_f\sqrt{k}$ as:

$$x_f\sqrt{k} = \frac{315.4T}{h\sqrt{\phi\mu_{gi}c_{ti}}} \cdot \frac{1}{\psi_i - \psi_{wf}} \cdot \frac{1}{m} \qquad \text{Equation 2-22}$$

where, m is the slope of the plot.

It was noticed that using the slope of the plot of $1/q_{gas}$ vs. $\sqrt{t}$ always tended to overestimate$x_f\sqrt{k}$. Ibrahim and Wattenbarger (2006) stated that the use of $1/q_{gas}$ vs. $\sqrt{t}$ led to estimation errors because of the pressure drawdown dependency of the linear flow system and, hence, proposed an empirical factor, f_c, which allows a more accurate determination of the $x_f\sqrt{k}$ value. Nobakht and Clarkson (2012) claimed that pseudo time should also be incorporated to account for the change of gas compressibility.

Traditionally, average viscosity and compressibility are estimated based on the average pressure across the entire reservoir, which may introduce estimation errors. Anderson and Mattar (2007) suggested that the calculations of the average viscosity and compressibility should be based on the average pressure within the region of influence. In this respect, $x_f\sqrt{k}$ could be calculated from the slope of $1/q_{gsc}$ vs. $\sqrt{t}_a$ plot using Equation 2-19. The accuracy of this traditional PDA technique has

been improved through correction by the ROI concept. They also found out that average pressure within ROI remains constant during the early transient period.

The traditional early PDA technique requires applications of pseudo variables. Vardcharragosad (2014) proposed a density-based solution for gas linear flow system under constant P_{wf} and the author developed a similar straight-line analysis technique. Without employing pseudo variables and using the plot of $1/q_{gsc}$ vs. t, $x_f\sqrt{k}$ could be calculated as

$$x_f\sqrt{k} = \frac{1}{\pi\sqrt{\alpha}_1}\frac{\rho_{sc}}{\rho_i}\frac{\sqrt{\mu_{gi}c_{gi}}}{h\sqrt{\phi}}\frac{\gamma_\rho\sqrt{\bar{\lambda}}}{\pi\sqrt{\pi}}\, m \qquad \text{Equation 2-23}$$

where $\gamma_\rho$is the density drawdown ratio defined as:

$$\gamma_\rho = \frac{\rho_i - \rho_{wf}}{\rho_i} \qquad \text{Equation 2-24}$$

$\bar{\lambda}$ is the pressure-dependent dimensionless ratio. As found by Anderson and Mattar (2007), the average reservoir pressure remains constant during the early transient period (under constant P_{wf} production). $\bar{\lambda}$ is a constant as has been shown in Vardcharragosad's work as well. Because the value of $\bar{\lambda}$ is related only to the initial pressure and the bottomhole pressure, one could simply obtain the value of $\bar{\lambda}$ using Vardcharragosad's early transient gas solution.

Previous PDA aims at extracting the $x_f\sqrt{k}$ value, assuming other reservoir properties are known. By contrast, this study is aiming at predicting BDF behavior without the knowledge of reservoir properties. A characterization ratio, $Y\sqrt{X}$, is used in the proposed BDF prediction model. In Vardcharragosad's study, this ratio can also

be calculated from the slope of the plot of $1/q_{gsc}$ vs. t. The density-based method could account for the change of gas compressibility without calculation of pseudo variables. The $Y\sqrt{X}$ ratio could be expressed as:

$$Y\sqrt{X} = \frac{2\sqrt{\bar{\lambda}}\, m}{\pi\sqrt{\pi}} \qquad \text{Equation 2-25}$$

2.4 Review of transition time determination and reservoir size estimation techniques

Transition time estimation is of great importance. It can be used as a tool to screen BDF window and it has been used to estimate OGIP in many previous studies (Watternbarger (1998); Arevalo et al, 2001 and 2005).

End of half slope is a simple method to screen the end of the early transient period and the beginning of BDF period of linear flow. In early transient period, log-log plot of $q_{gsc}\ vs.\ t$ would yield a straight line with -0.5 slope and log-log plot of $G_P\ vs.\ t$ would yield a straight line with 0.5 slope. The time when log-log plot of $q_{gsc}\ vs.\ t$ deviates from -0.5 slope straight line or when the log-log plot of $G_P\ vs.\ t$ deviates from 0.5 slope, should be the transition time t_e. This method is simple, however, not accurate enough. Determination of the end of half slope on a log-log plot is arbitrary and may yield different results. It's also hard to spot the $t_e$on a log-log plot.

Watternbarger (1998) also suggested that many wells may be shut off or occasionally experience changes in well pressure because of market curtailment. When this was happening, the half slope may not always be apparent or may remain

steady. The end of half slope method should be seen as a screening method rather than a quantitative tool for analysis.

Recently, a new approach of determining the transition time from early to boundary-dominated conditions was presented by March et al. (2016). This study applied their findings to a countercurrent spontaneous invasion process. Spontaneous invasion of a wetting phase into a porous system driven by capillary force is a physical process that is common in many geological applications. This process could also be considered in two stages: early time stage and late time stage. During the early time stage, the advance of the wetting phase front has not reached the no flow boundary, which is shown in Figure 2.5 as L_c (the black dash line). The early time behavior is characterized by an analytical solution scale based on $\sqrt{t}$ (Lucas, 1918; Washburn, 1921) During a late time stage, imbibition has reached the boundary L_c and the late time behavior follows the empirical exponential model given by Aronofsky et al. (1958):

$$\frac{V}{V_\infty} = 1 - e^{-\lambda t} \qquad \text{Equation 2-26}$$

where λ represents the rate of the transfer.

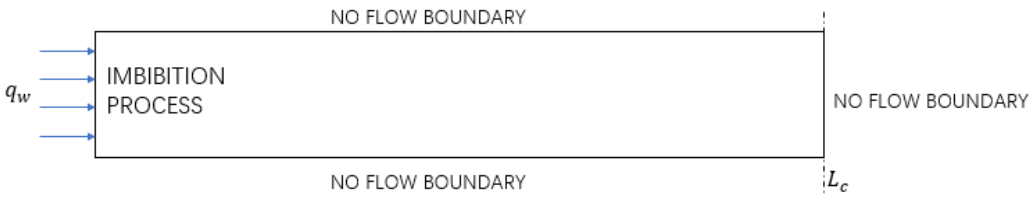

Figure 2-4 Graphical representation of single dimension counter-current spontaneous imbibition

March et al. (2016) presented a hybrid model of imbibed volume based on existing early time analytical model and late time empirical model. While formulating the hybrid model, transition time of early time behavior and late time behavior need to be determined first.

The process of determining the transition time is called “filling-back procedure” by March et al. (2016). The analytical profile of water saturation shown in Figure 3-8 is for a semi-infinite domain, which means it is only suitable for early time before the imbibition process reaches the boundary. For the reason that analytical solution is only available for early stage, overall saturation when the no flow boundary is reached could not be obtained. In this case, the “filling-back procedure” uses the saturation profile of early stage to determine the transition time. Basing on the early time analytical profile, they proposed a mass conservative method to catch the transition time, t. They took the imbibed volume that had left the no flow boundary according to the analytical solution and filled it back into the domain. This was accomplished by filling back the shadow area on the right side of the boundary to the shadow area on the left side (the area of the green shadow part on the left side of the boundary in Figure 2.6 should equal the area on the right-side shadow). A saturation plateau (S_w) that leads to an equivalent volume in the physical domain need to be identified to conduct the filling back procedure. The time when the two shadows have the same area is defined as the transition time.

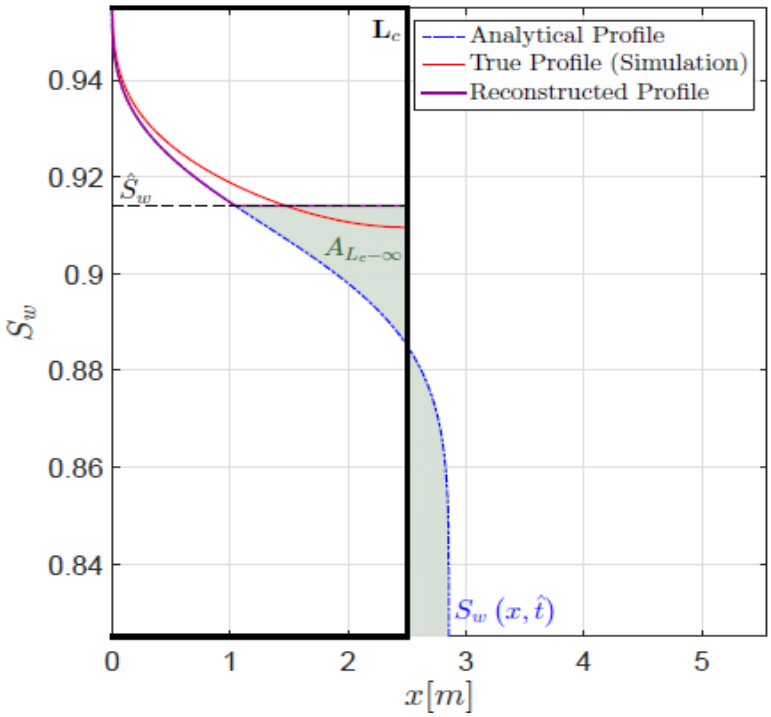

Figure 2-5 Filling back procedure (March et al., 2016)

The notions of early time and late time behaviors are very similar to how we define early transient flow and late boundary-dominated flow in linear flow system. In the methodology section, we show how we apply this approach to dry gas production.

2.5 Review of BDF gas solution – under constant P_{wf}

Classical linear flow system could be a vertical well with an infinite conductivity fracture that extends to reservoir drainage boundaries or a horizontal well with multi-stages fractures. In such situations, the diffusivity equation for linear flow systems in pseudo-function form could be expressed as:

$$\frac{\partial^2 \psi}{\partial r^2} = \frac{\phi \mu_{gi} c_{ti}}{k} \frac{\partial \psi}{\partial t_a} \qquad \text{Equation 2-27}$$

ψ and $t_a$denote pseudo pressure and pseudo time：

$$\psi = \int_0^p \frac{2p}{\mu_g z} dp \qquad \text{Equation 2-28}$$

$$t_a = \int_0^t \frac{\mu_{gi} c_{gi}}{\mu_g c_t} dt \qquad \text{Equation 2-29}$$

Miller (1962) derived solutions for the case of unsteady influx of water in linear aquifer reservoirs by modifying Carslaw and Jaeger's (1959) heat transfer solution: for a linear closed boundary reservoirs produced under a constant P_{wf} condition, the liquid solution to the linear PDE can be written as an infinite series:

$$q_D = \frac{4}{\pi} \cdot \frac{x_f}{r_e} \sum_{n_{odd}}^{\infty} exp\left(-\frac{n^2\pi^2}{4} \cdot (\frac{x_f}{r_e})^2 t_D\right) \qquad \text{Equation 2-30}$$

The definitions of the dimensionless variables for the liquid are as shown in Equations 2-3 and 2-4. This liquid solution could also be written in decline dimensionless form:

$$q_{Dd} = \sum_{n_{odd}}^{\infty} exp(-n^2 t_{DAd}) \qquad \text{Equation 2-31}$$

The definition of dimensionless decline variables are defined as:

$$q_{Dd} = \frac{\pi r_{eD}}{4} q_D \qquad \text{Equation 2-32}$$

$$t_{DAd} = \frac{\pi^2}{4 r_{eD}^2} t_D \qquad \text{Equation 2-33}$$

r_{eD} is dimensionless size of reservoir and in the linear flow system, it is defined as:

$$r_{eD} = \frac{r_e}{x_f} \quad \text{Equation 2-34}$$

Watternbarger et al. (1998) then adapted the linear liquid solution to gas flow by replacing pressure by pseudo-pressure. They argued that the above liquid solution could be transformed into gas solution by writing dimensionless variables in terms of the pseudo functions as:

$$q_D = \frac{P_{sc}}{\alpha_1 \pi T_{sc}} \frac{q_{gsc} T}{kh(\psi_i - \psi_{wf)}} \quad \text{Equation 2-35}$$

$$t_D = \frac{\alpha_1 k t_a}{\phi \mu_{gi} c_{ti} {x_f}^2} \quad \text{Equation 2-36}$$

A density-based transformation of liquid solution to gas solution for radial flow was proposed originally by Ye and Ayala (2012). Density-based approaches allow us to obtain gas solutions produced under constant P_{wf} production by implementing a $\bar{\lambda}$-$\bar{\beta}$ rescaling as:

$$q_D^{gas}(t_D) = \bar{\lambda} \cdot q_D^{liq}(\bar{\beta} t_D) \quad \text{Equation 2-37}$$

Vardcharragosad (2014) has shown that the density-based transformation in Equation 2-37 could be extended to linear flow regime. Linear gas solution could be obtained by applying $\bar{\lambda}$ and $\bar{\beta}$ rescaling method. Equation 2-31 and 2-32 could be transformed into:

$$q_{Dd} = \frac{4\bar{\lambda}}{\pi} \cdot \frac{x_f}{r_e} \sum_{n_{odd}}^{\infty} exp\left(-\frac{n^2\pi^2}{4} \cdot (\frac{x_f}{r_e})^2 \, \bar{\beta} t_D\right)$$ Equation 2-38

$$q_{Dd} = \bar{\lambda} \sum_{n_{odd}}^{\infty} exp\left(-n^2 \, \bar{\beta} t_{DAd}\right)$$ Equation 2-39

The definitions of pressure-dependent variables $\bar{\lambda}$ and $\bar{\beta}$ have already been provided through Equations 2-12 and 2-23, respectively, and the average density in a reservoir can be determined on the basis of the material balance statement (assuming volumetric dry gas depletion):

$$\frac{\bar{\rho}}{\rho_i} = (1 - \frac{G_p}{OGIP})$$ Equation 2-40

where G_p denotes cumulative gas production:

$$G_p = \int_0^t q_{gsc} \, dt$$ Equation 2-41

and OGIP denotes original gas in place and is calculated as:

$$OGIP = \frac{4 r_e x_f h \phi}{B_{gi}}$$ Equation 2-42

The rescaled infinite series solution is rigorous, but it may not be found to be sufficiently satisfying for production data analysis purposes due to the presence of infinite number of terms. Vardcharragosad (2014) truncated the rescaled infinite series in Equation 2-39 to get a 'long-time approximation solution' (LTA) for BDF in terms of dimensionless decline flow rate and decline time:

$${q_{Dd}}^{*gas,LTA} = \bar{\lambda} \cdot \exp\left(-\bar{\beta} {t_{DAd}}^*\right)$$ Equation 2-43

This solution keeps the first term (n=1) in equation 2-27. It should be accurate during late-time with accurate $\bar{\lambda}$ and $\bar{\beta}$ values used because when t_{DAd} is big enough so the rest of the infinite series could be omitted. However, it should fail to capture early time production rate, because when $t_{DAd}$is small, the infinite series could not be omitted. Due to the mismatch of flow rate during early transient period, material balance equation as shown in equation 2-39 is not guaranteed. In this condition, the average density of the reservoir for the determination of $\bar{\lambda}$ and $\bar{\beta}$ will be estimated incorrectly in the LTA approach, which results in inaccurate prediction of late time behaviors as well. Therefore, to ensure more accurate results, the proposed LTA approach needs a material balance correction.

Vardcharragosad also derived a "Material balance BDF solution'' (or MB-BDF solution) by using the following gas diffusivity equation:

$$q_{Dd}{}^{*gas,LTA} = \bar{\lambda} \cdot \frac{3}{2}\, exp\left(-\frac{12}{\pi^2}\bar{\beta} t_{DAd}{}^{*}\right) \qquad \text{Equation 2-44}$$

Unlike LTA, the MB-BDF solution follows the reservoir material balance statement strictly but assumes that BDF starts at the very beginning of production, which is not possible. Therefore, the MB-BDF solution results in a mismatch when boundary-dominated behavior begins just as it is trying to preserve material balance. The LTA solution is not accurate as well because of improper $\bar{\lambda}$ and $\bar{\beta}$ calculation due to the failure of preserving material balance. Vardcharragosad has shown that the best match could be obtained by using the LTA solution with a material balance adjustment that could be accomplished in either of the ways described below:

1) Implementing the LTA solution and the MB-BDF solution together. The MB-BDF solution is simply used for estimating accurate $\bar{\lambda}$ and $\bar{\beta}$ values.

2) Adjusting the LTA cumulative production by a factor $\frac{\pi^2}{8} \approx 1.23$, also for the purpose of estimating accurate $\bar{\lambda}$ and $\bar{\beta}$ values.

In Vardcharragosad's study, it was demonstrated that the rescaled gas solution has a best match with numerical simulation, whereas LTA with MB adjustment gives a relatively good result compared to LTA and MB-BDF solution. Hence, we will develop BDF prediction approach based on the rescaled gas solution and LTA with MB adjustment.

CHAPTER 3 - METHODOLOGY

This chapter begins with descriptions of two techniques for estimating the transition time and the reservoir size: one of the methods used both gas flow rate and cumulative gas production while the other method is called the "Analogous Filling-back Procedure" which is inspired by a transition time determination approach in a countercurrent spontaneous imbibition process. Then a PDA method is presented which also uses both gas flow rate and cumulative gas production. The proposed BDF model is based on Vardcharragosad's (2014) long-term approximation BDF model with material balance adjustment. Using transition time determination and PDA techniques, the BDF prediction model was built.

3.1 Using product of q_{gsc} and G_p

As stated in Section 2.4, using the end of half slope in the q_{gsc} plot always tends to underestimate t_e whereas using end of slope by G_p tends to overestimate t_e. Here I proposed to explore a numerically generated production data produced from a synthetic reservoir as an example. Firstly, I define a variable called the actual transition time, $t_{e,a}$.

The purpose of the determination of t_e is to estimate reservoir size as:

$$r_e = C_r \cdot \left(\frac{\alpha_1 k t_e}{\phi \mu_{gi} c_{gi}}\right)^{0.5} \qquad \text{Equation 3-1}$$

To have an accurate estimation of r_e, an accurate value of t_e is crucial. In the numerical case study, the actual transition time $t_{e,a}$ is defined by inversely calculating inputs to our synthetic reservoirs and the C_r value of 2.554 suggested by

Nobakht and Clarkson (2012) for linear flow under constant bottomhole pressure specification.

Table 3-1 Input of a sample study

Input	Value
Pi(psi)	5000
Pwf(psi)	3220
T (F)	290
sg	0.717
Porosity	0.15
k (md)	0.01
Thickness (ft)	92
Xf(ft)	392.7
re(ft)	2000

The numerically generated data for the input shown in Table 3-1 is used to validate the methodology. $t_{e,a}$ is calculated to be 1051 days. As we have stated in the Chapter 2, the use of the traditional end of half slope method to determine transition time causes significant errors. Figure 3-1 shows that the end of half slope method, t_e obtained from log-log plot of G_P $vs.t$ is 2000 days and from log-log plot of q_{gsc} $vs.t$ is 600 days. We again conclude that the use of the log-log plot of q_{gsc} $vs.t$ significantly underestimated t_e whereas using the log-log plot of G_P $vs.t$ has overestimated t_e.

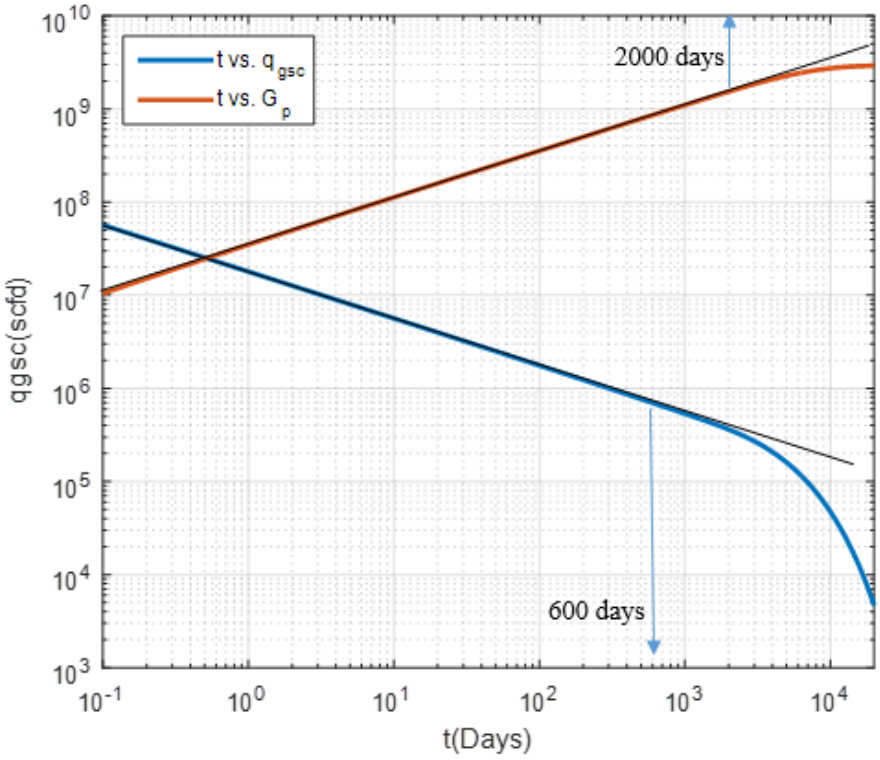

Figure 3-1 Illustration of End of half slope method (A numerical case)

Since using q_{gsc} underestimates t_e while using G_P overestimates t_e, numerically couple these two parameters may potential offer the accurate estimates. The dimensionless cumulative gas production can be calculated as:

$$G_{PD} = \int_0^t q_D dt_D = \frac{4\sqrt{\bar{\lambda}}}{\pi\sqrt{\pi}}\sqrt{t_D} \qquad \text{Equation 3-2}$$

By inspecting the expressions for q_D and G_{PD} for the early transition period, it was noted that the product of q_D and G_{PD} is independent of time:

$$q_D \cdot G_{PD} = \frac{8\bar{\lambda}}{\pi^3} \qquad \text{Equation 3-3}$$

Writing the above equation in terms of real gas flow rate and cumulative gas production:

$$q_{gsc} \cdot G_p = \left(\alpha_1 \frac{2\pi kh\mu_{gi}c_{gi}(\rho_i - \rho_{wf})}{\rho_{sc}}\right)^2 \cdot \frac{\alpha_1 k}{\phi\mu_{gi}c_{gi}x_f^2}\frac{8\sqrt{\bar{\lambda}}}{\pi^3} =$$

Equation 3-4

$$\text{constant} \cdot \sqrt{\bar{\lambda}}$$

The $\bar{\lambda}$ value is the average viscosity-compressibility dimensionless ratio between average reservoir pressure and bottom-hole pressure and it is a function of initial reservoir pressure and bottomhole pressure. Hence, one can simply calculate the $\bar{\lambda}$ value using Vardcharragosad's early transient model. According to Anderson and Mattar (2007), the average pressure within ROI remains constant during the early transient period, so $\bar{\lambda}$ value remains constant; which indicates that $q_{gsc} \cdot G_p$ should remain constant during the early transient period. The time when $q_{gsc} \cdot G_p$ deviates from constant should be the transition time, t_e, we can apply it for our late-BDF prediction.

As shown in Figure 3-2, the product of q_{gsc} and G_p remains constant before around 1000 days, but after 1000 days the product begins to decline. Comparing this with the accurate transition time, which is 1051 days, the estimated error is 4.87% which is believed to be acceptable. In all cases, it is superior to end of half slope method because the improved accuracy.

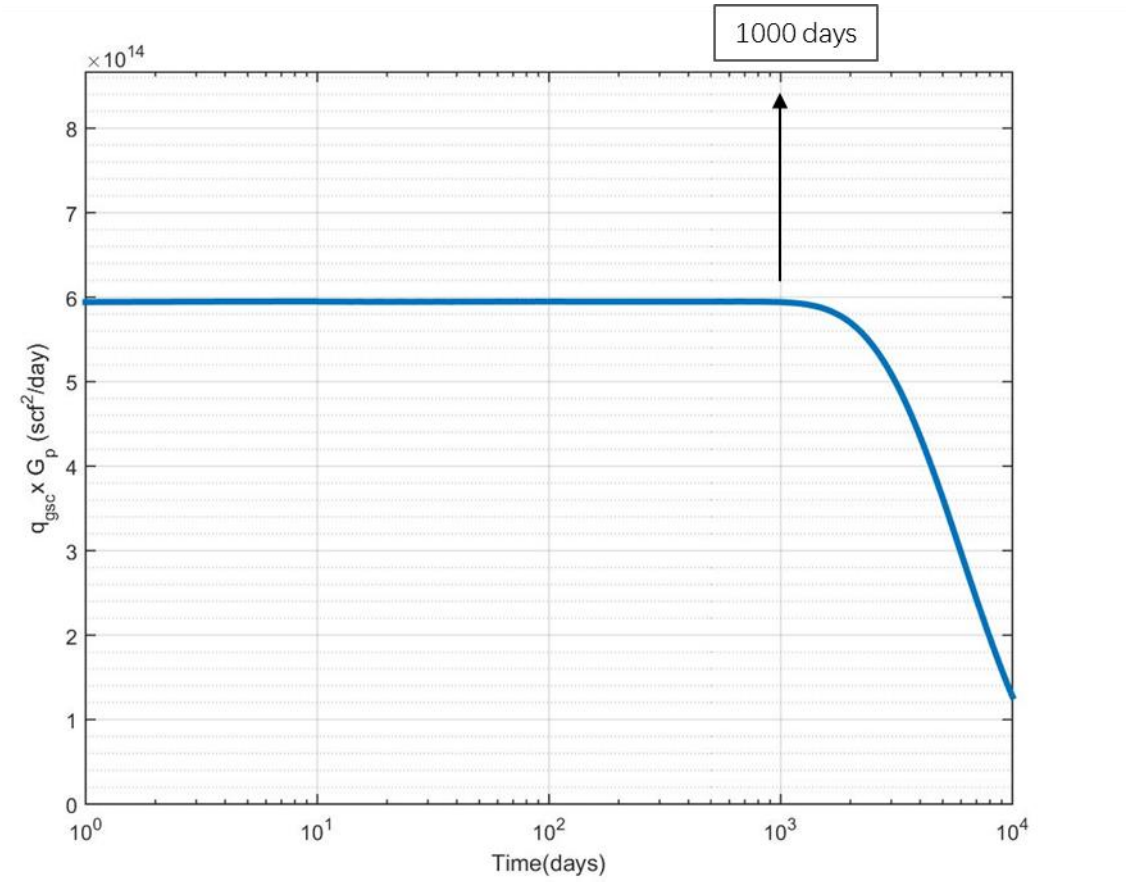

Figure 3-2 Transition Time Determination Using Product of $\boldsymbol{q_{gsc}}$ and $\boldsymbol{G_p}$

3.2 Determination of transition time – Analogous Filling Back Procedure

March et al. (2016) developed a new method to determine transition time of a countercurrent spontaneous invasion process. In the invasion process, the time before the advance of the wetting phase front influencing the no-flow boundary is called the early time and after the wetting phase front reaches the boundary, it is called the late time. The notions of early time and late time behaviors are very similar to how we define early transient flow and late boundary-dominated flow in linear flow system. March et al. had used water saturation to characterize transition time. In dry gas production case, the same approach was adopted to determine transition times. Similar to water saturation in March's filling back procedure, I chose the pressure at

the reservoir boundary as the criterion for characterizing the transition time. According to the numerical simulation results and analytical solutions, the pressure decline at the reservoir boundary when BDF starts is found to be around 7%. Therefore, the transition time could be determined using an analogous filling back procedure. The early transient pressure solution under constant bottomhole pressure constraint is given by:

$$P_D(r_D, t_D) = erfc(\frac{r_D}{2\sqrt{t_D}}) \quad \text{Equation 3-5}$$

where $P_D = \frac{P_i - P(r_D, t_D)}{P_i - P_{wf}}$

The black solid line in Figure 3-3 represents the profile for infinite domain (early time pressure profile). Following the use of a Cr value of 2.554 and Vardcharragosad ‘s NPD theory as shown in Equation 2-21, it is found that the pressure at the outer reservoir boundary is 93% of initial reservoir pressure when boundary-dominated flow regime begins. As shown in Figure 3-3, we can now accomplish the mass conservative method in terms of pressure. The blue line represents reservoir boundary and area of region A and region B should be equal when BDF behavior begins.

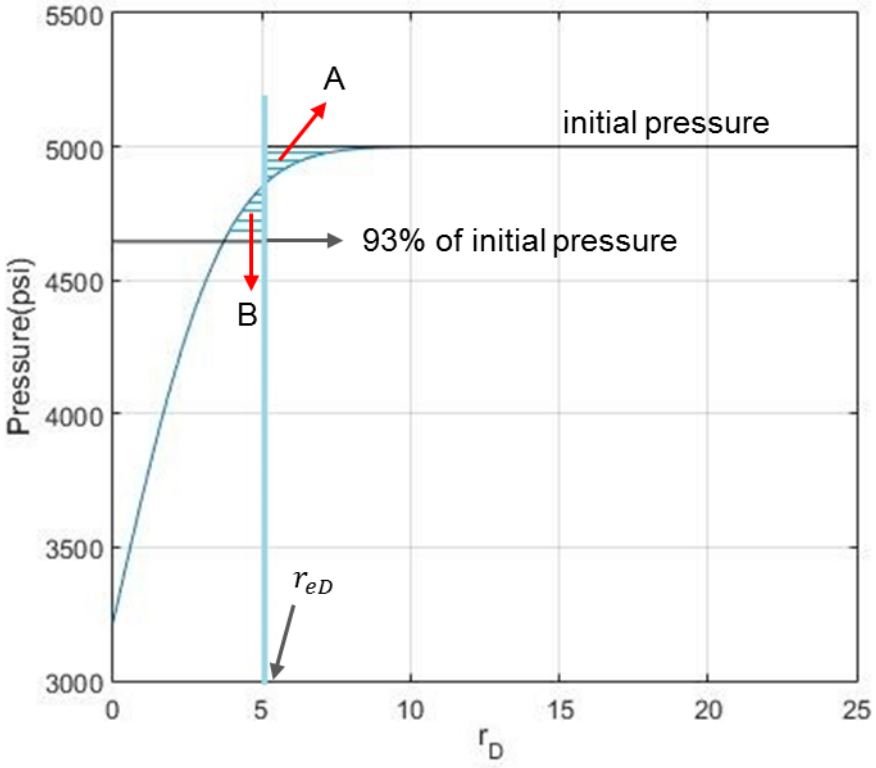

Figure 3-3 Analogous filling back procedure

Although production data after BDF window is not required in this analogous filling back procedure, it requires knowledge of some reservoir properties. Before the analysis, r_{eD} (r_e/x_f) value is required to define areas of shadow A and B. In order to transform t_{eD} (dimensionless time) to t_e (real transition time) using definition of dimensionless time as shown in Equation 2-13, value of $\frac{\alpha_1 k}{\phi \mu_{gi} c_{gi} {x_f}^2}$ is also required. Using the value of $Y\sqrt{X}$, one could also use *h* and *k* to obtain the value of $\frac{\alpha_1 k}{\phi \mu_{gi} c_{gi} {x_f}^2}$. This analogous filling-back procedure shows big limitation. In the next section, I'll introduce another method to determine transition time without such limitation.

3.3 Production data analysis techniques

Another rate-time analysis approach was developed here by combining gas flow rate with cumulative gas production. As already shown in section 3.1, the product of q_{gsc} and G_p remains constant during early transient period:

$$q_{gsc} \cdot G_p = \left(\frac{\alpha_1 2\pi kh(\rho_i - \rho_{wf})}{\rho_{sc}\mu_{gi}c_{gi}}\right)^2 \cdot \frac{\phi\mu_{gi}c_{gi}x_f^2}{\alpha_1 k}\frac{8\sqrt{\bar{\lambda}}}{\pi^3} = C \cdot \sqrt{\bar{\lambda}} \quad \text{Equation 3-6}$$

The above equations suggest that the product of gas flow rate and cumulative gas production should remain constant during the early-transient period. Since the value of $\bar{\lambda}$ has been shown to remain constant for constant P_{wf} gas production under a linear flow regime during early transient period, the value of C may be calculated directly as:

$$C = \frac{4\sqrt{2}\sqrt{\alpha_1}}{\rho_{sc}\sqrt{\mu_{gi}c_{gi}}\sqrt{\pi}} \cdot \phi x_f^2 h^2 k = \frac{q_{gsc} \cdot G_p}{\sqrt{\bar{\lambda}}} \quad \text{Equation 3-7}$$

$Y\sqrt{X}$ can be expressed in terms of *C* as:

$$Y\sqrt{X} = \frac{2\sqrt{2}(\rho_i - \rho_{wf})}{\pi\sqrt{\pi}\rho_i\sqrt{C}} \quad \text{Equation 3-8}$$

As stated in last section, the $Y\sqrt{X}$ value will be used in our proposed BDF prediction. A correct $Y\sqrt{X}$ ratio can be calculated as comparison when reservoir properties are known:

$$Y\sqrt{X} = \frac{1}{2\pi\sqrt{\alpha_1}}\frac{\rho_{sc}}{\rho_i}\frac{1}{h\sqrt{\phi}}\sqrt{\mu_{gi}c_{gi}}\cdot\frac{1}{x_f\sqrt{k}} \qquad \text{Equation 3-9}$$

I took a numerically generated case based on inputs as an example (see Table 3-1). As shown in Figure 3-4, during the early transient period, the product of flow rate and the cumulative is constant at 5.95e14. Using Equation 3-8, the characterization ratio $Y\sqrt{X}$ is found to be 5.331e-9. The correct $Y\sqrt{X}$ ratio calculated by Equation 3-9 is 5.328e-9. It was found that, the proposed rate-time analysis method successfully estimates $Y\sqrt{X}$ with a very small error in this hypothetical numerical case. More case studies will be presented in Chapter 4 to further validate this approach.

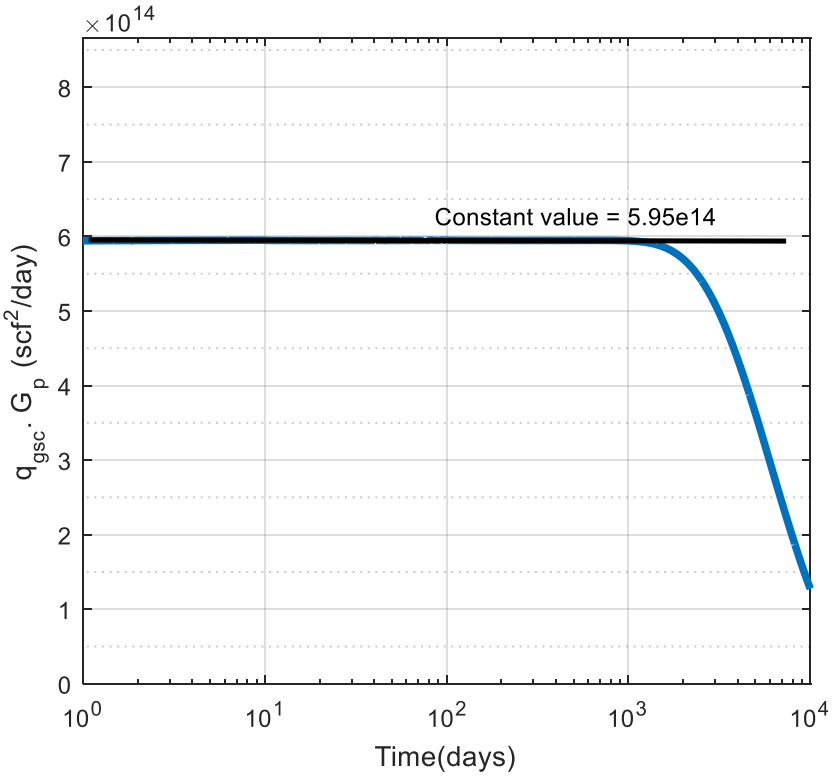

Figure 3-4 Proposed method of early rate-time analysis (Example Case)

3.4 Development of BDF prediction

Vardcharragosad's current study involves the constant-P_{wf}gas solution for the classical linear flow system for both the early transient period and the boundary-dominated period as well as rate-time analysis of early-transient flow data. In reality, the precise reservoir properties are normally unknown. In this section, I will describe how to use early production data to predict boundary-dominated flow behavior without detailed reservoir properties.

Two procedures are used to make the prediction:

1. Determine the characteristic ratio $Y\sqrt{X}$: This could be accomplished by rate-time analysis of early data, as shown in Section 3.3.
2. Find the end of the linear transient period t_e: this could be accomplished by either of the following two methods:
    a. Using the end of half slope method: The plot of gas flow rate q_{gsc} vs. t in log-log scale should yield a negative half slope. Integration of $q_{gsc}$with respect to *t* estimates the cumulative production. The result is a plot of G_p vs. t in log-log scale with a positive half slope.
    b. Combine q_{gsc} and G_p: Determine the transition time when the product of q_{gsc} and G_p deviates from constant, as shown in Section 3.3.

Once the characteristic ratio $Y\sqrt{X}$ and t_e are determined, these two values can be used as inputs to do the BDF prediction using the following proposed method. Our

BDF prediction for linear gas flow is based on rescaled general solution. The rescaled general solution for gas is expressed as:

$$q_{Dd} = \sum_{n_{odd}}^{\infty} exp(-n^2 t_{DAd}) \quad \text{Equation 3-10}$$

Replacing the dimensionless decline flow rate and the decline time by the real flow rate and time values,

$$q_{gsc} = \frac{4}{\pi r_{eD}} \frac{r_\rho}{Y} \bar{\lambda} \cdot \sum_{n_{odd}}^{\infty} exp\left(-\frac{\pi^2}{4 r_{eD}^2} X \bar{\beta} t\right) \quad \text{Equation 3-11}$$

Using the radius of investigation concept:

$$r_{eD} = C_r \cdot \left(\frac{\alpha_1 k t_e x_f^2}{\phi \mu_{gi} C_{gi}}\right)^{0.5} \quad \text{Equation 3-12}$$

From Equation 2-4 and Equation 2-5 we get the expressions for X and Y. Substituting X, Y and r_{eD} into Equation 3-12:

$$q_{gsc} = \bar{\lambda}\, r_\rho \frac{4}{\pi} \frac{1}{C_r \sqrt{t_e}} \frac{1}{Y \sqrt{X}} \sum_{n_{odd}}^{\infty} exp\left(-\frac{\pi^2}{4} \frac{1}{C_r^2 t_e} \bar{\beta} t\right) \quad \text{Equation 3-13}$$

Pressure-dependent variables $\bar{\lambda}$ and $\bar{\beta}$ are calculated based on reservoir average density and it is calculated from the overall material balance statement:

$$\frac{\bar{\rho}}{\rho_i} = (1 - \frac{G_p}{OGIP}) \quad \text{Equation 3-14}$$

Cumulative gas production is calculated as:

$$G_p = \int_0^t q_{gsc}\, dt \quad \text{Equation 3-15}$$

Therefore, flow rate calculated from Equation 3-6 is our prediction for the BDF behavior when Equation 3-14 is used to evaluate reservoir average pressure and calculate $\bar{\lambda}$ and $\bar{\beta}$. The proposed BDF prediction method only requires knowledge of gas specific gravity, reservoir temperature, initial reservoir pressure, and imposed bottomhole flowing pressure, which are normally available to the operator. Values of permeability, reservoir outer boundary location, half fracture length, and reservoir thickness are not required.

As demonstrated in the preceding section, $\bar{\lambda}$ and $\bar{\beta}$ are pressure-dependent variables. In order to accurately evaluate $\bar{\lambda}$ and $\bar{\beta}$, the material balance was used to obtain reservoir average pressure. In this ideal linear flow system where fractures extend to the reservoir boundaries, as depicted in Figure 2-2, the OGIP can be estimated as:

$$OGIP = \frac{4x_f h\phi r_e}{B_{gi}} \qquad \text{Equation 3-16}$$

OGIP can be expressed in terms of t_e and $Y\sqrt{X}$, the deviation of OGIP estimation is shown in Appendix C:

$$OGIP = \frac{4x_f h\phi r_e}{B_{gi}} = \frac{4\sqrt{t_e}}{Y\sqrt{X}} \Big/ \left(\frac{2\pi}{C_r}\right) \qquad \text{Equation 3-17}$$

Based on the recommendations of Nobakht and Clarkson (2012a), the use of a Cr-value of 2.554 is reasonable while calculating the ROI for a classical linear flow system with constant P_{wf}. The OGIP thus calculated is used for density calculation—as shown in the material balance statement expressed by Equation 3-84. To validate the proposed BDF prediction method, a case study was investigated with

the inputs shown in Table 3-1. Fluid properties in this case study and all numerical studies in this thesis are calculated using Lee et al (1966) for gas viscosity, Dranchuk and Abou-Kassem (1975) for Z-factor, Abou-Kassem et al (1990) for C_g.

Figure 3-5 shows that our proposed BDF prediction method could fully match Vardcharragosad's gas BDF model using the transition time.

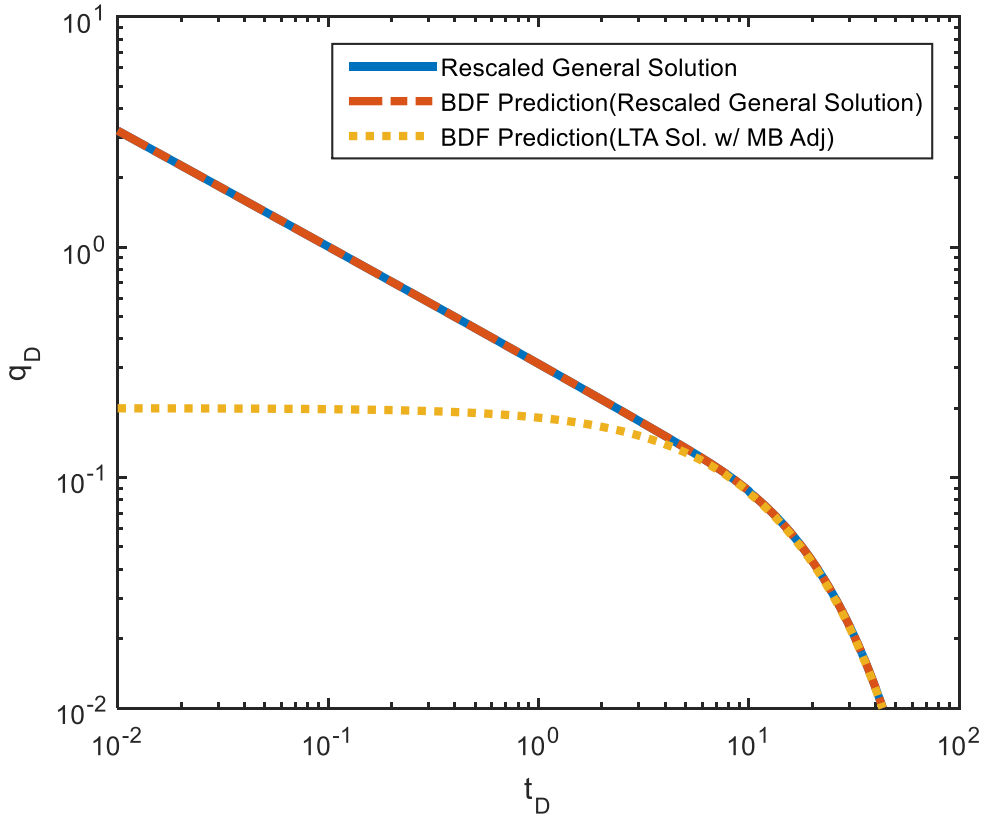

Figure 3-5 Comparison of Vardcharragosad's gas model and Our proposed BDF prediction

The BDF prediction based on rescaled LTA solution for gas is expressed as:

$$q_{gsc} = \bar{\lambda}\, r_\rho \frac{6}{\pi} \frac{1}{C_r\sqrt{t_e}} \frac{1}{Y\sqrt{X}} exp\left(-\frac{3}{C_r^2 t_e}\bar{\beta}t\right) \quad \text{Equation 3-18}$$

The BDF prediction based on rescaled LTA solution for gas is expressed as:

$$q_{gsc} = \bar{\lambda}\, r_\rho \frac{4}{\pi}\ \frac{1}{C_r\sqrt{t_e}}\ \frac{1}{Y\sqrt{X}}\ exp\left(-\frac{\pi^2}{4}\frac{1}{C_r^2 t_e}\bar{\beta}t\right) \qquad \text{Equation 3-19}$$

From comparison of all the solutions, other than the rescaled general solution, the hybrid approach that implements the LTA solution but with material balance adjustment to calculate $\bar{\lambda}$ and $\bar{\beta}$ gave a relatively accurate forecasting as well.

Example of BDF prediction:

In this example, numerically generated data for linear flow conditions is based on inputs shown in Table 3-1.

Step 1: $\bar{\lambda}$ calculation:

Since $\bar{\lambda}$ value only depends on initial reservoir pressure and imposed buttomhole pressure and remains constant during early transient flow, one could obtain this value by employing Vardcharragosad's gas model as shown in Equation 2-15. In this example study, $\bar{\lambda}$ is calculated to be 0.731.

Step 2: Early data analysis:

Plot $q_{gsc} \cdot G_p$ vs. t as shown in Figure 3-6. The product remains a constant value of 5.95e14 before reaching BDF window. $Y\sqrt{X}$ is calculated to be 5.32E-09 using this constant value and the $\bar{\lambda}$ value calculated from step 1 using Equation 3-6 and Equation 3-7. Compared to the correct $Y\sqrt{X}$ value - 5.33E-9, which is calculated from the definition of the multipliers X and Y, the proposed data analysis shows high accuracy.

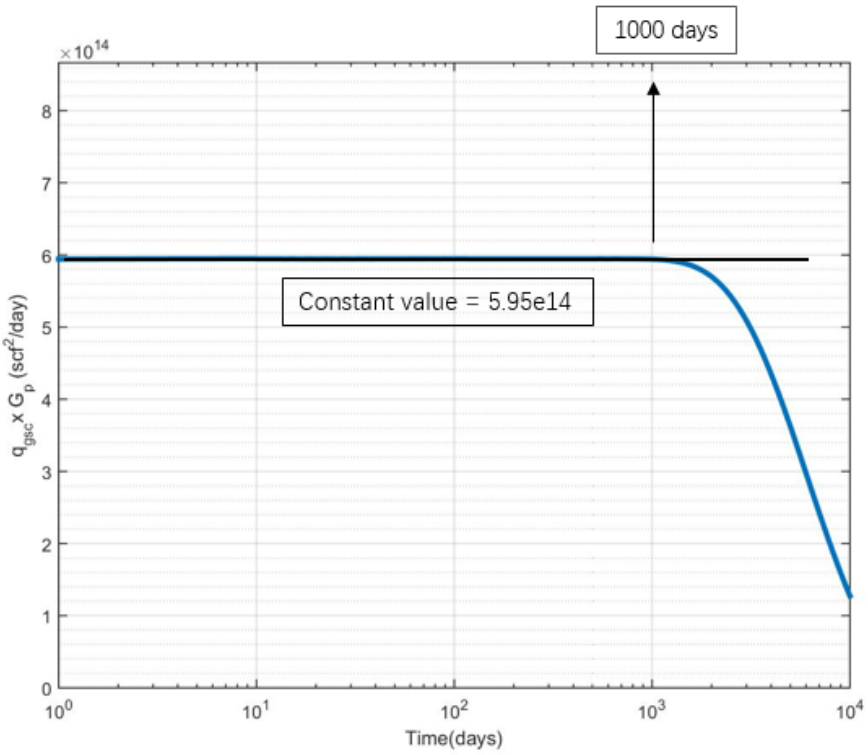

Figure 3-6 Plot of $q_{gsc} \cdot G_p$ vs. t – Example case

Step 3: Transition time determination:

a. If production data after BDF window is available, same plot could be used identify t_e. In this example study, as shown in Figure 3-6, the product of q_{gsc} and G_p starts to deviate from constant value at around 1000 days.

b. If production data after BDF window is not available, the analogous filling back procedure is used to determine t_e. The analogous filling-back procedure will require the knowledge of r_{eD} or one of the following sets of reservoir properties: 1) k, ϕ, x_f 2) h, k. Calculate pressure profile using Equation 3-5 at different t_D. For efficiency, use program to find the time when area A and area B equals. The plot $t_{eD}$is found is shown in Figure 3-

7. In this example case, t_{eD} is found to be 4.2. Using available reservoir properties, t_e is calculated to be 1102 days.

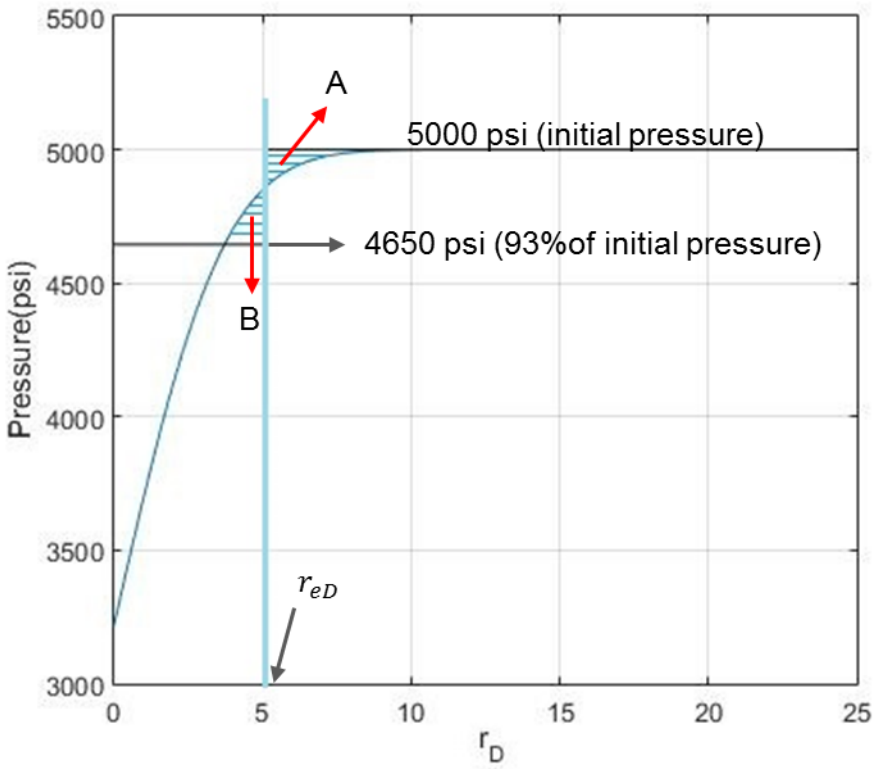

Figure 3-7 Analogous filling back procedure

Step 4: OGIP calculation

OGIP is calculated using $Y\sqrt{X}$ and t_e determined from Step 2 and 3 as:

$$OGIP = \frac{4\sqrt{t_e}}{Y\sqrt{X}} / \left(\frac{2\pi}{C_r}\right) \qquad \text{Equation 3-20}$$

As mentioned in Step 1, error of $Y\sqrt{X}$ determination in this sample study is very small. The error of OGIP determination largely results from error of t_e. In Table 3-2 we compare differences from using end of half slope and using the hybrid method. Using end of half slope (q_{gsc} plot) significantly underestimates t_e whereas using G_p plot significant

overestimates t_e and both causes big error in OGIP calculation. The hybrid method and analogous filling-back procedure show great advantage overs the traditional end of half slope method. In next Chapter, I will further test the accuracy of proposed t_e determination techniques with more case studies.

Eample study				
	End of half slope q_{gsc}	End of half slope G_p	Hybrid method $q_{gsc} \cdot G_p$	Analogous FB Procedure
t_e	-33.41%	90.25%	-4.87%	4.80%
OGIP	-18.28%	38.13%	-2.32%	2.52%

Table 3-2 Comparison of error - example study

Step 5: BDF gas rate forecasting

Use the proposed BDF prediction solution as shown in Equation 3-13 to forecast BDF behavior. The detailed procedure is shown in Appendix D. The result of BDF prediction is shown in Figure 3-8. With smaller errors in two proposed t_e determination techniques, the BDF gas rate is well predicted. As expected, end of half slope method cause big errors in t_e determination, thus results inaccurate BDF gas rate prediction.

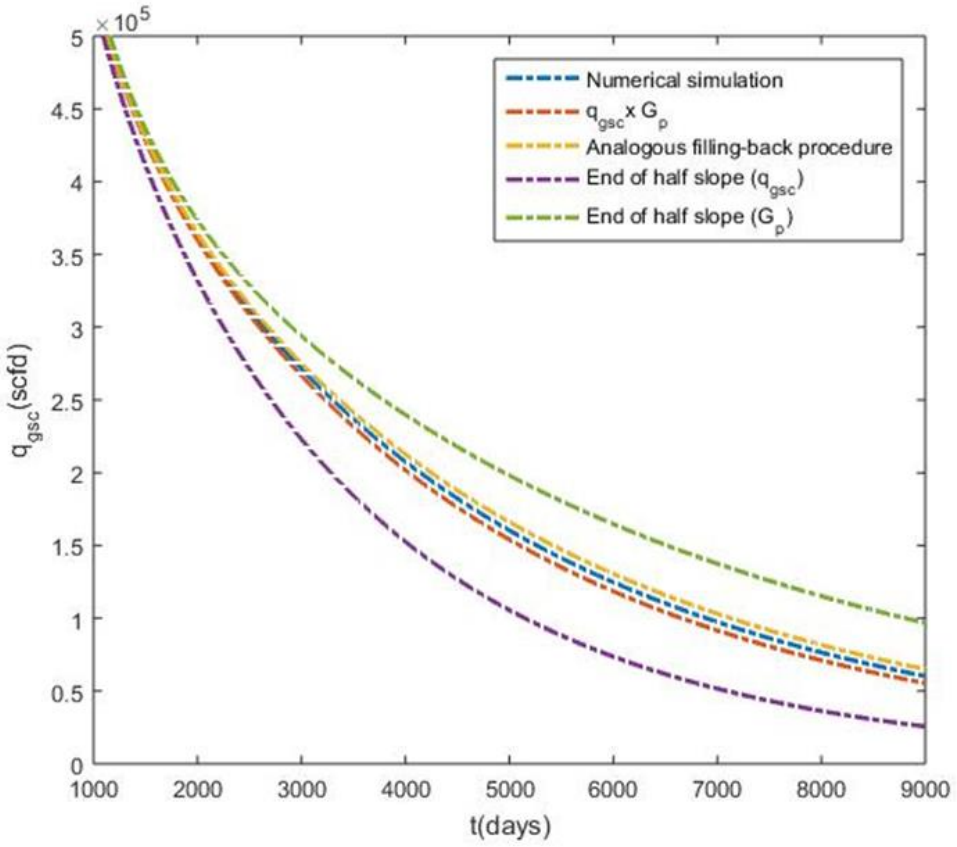

Figure 3-8 BDF gas rate prediction - example study

This chapter firstly shows approaches to get more accurate estimations of t_e. Using the product of q_{gsc} and G_p, errors from two end of half slope methods could be cancelled out and the accuracy of estimations of t_e has been significantly improved. The analogous filling-back procedure also provides more accurate result compared to end of half slope. An accurate $Y\sqrt{X}$ ratio could be determined using the constant value of the product of q_{gsc} and G_p. Using t_e and $Y\sqrt{X}$, I am able to make BDF prediction without knowing detailed reservoir properties. Also, OGIP could directly calculated using these two values.

CHAPTER 4 - Case Studies

In this section, a mix of 64 synthetic cases and 3 field cases are investigated to test the validity of the proposed methodology. For 64 synthetic reservoir production profiles, commercial software package CMG-IMAX® was used to generate numerical production data. All the synthetic reservoirs were generated based on a 1D linear system with homogeneous and isotropic reservoir properties. All were discretized using a logarithmic grid size distribution from the well bore location to the reservoir boundary. The reservoir is drained by a fully penetrating well, placed at its center and produces under constant bottom-hole pressure specification. The inputs for the 64 synthetic cases are shown in Table 4-1. More detailed input specifications are presented in Appendix A. To further test the applicability of the methodology, 3 field-based case studies—Coapa A well, Dakota well A, and Ca-31 well—will also be presented in this chapter.

Input	Value
Pi(psi)	5000, 4000
Pwf(psi)	3220, 1810
T (F)	290
sg	0.717
Porosity	0.15
k (md)	0.05, 0.01
Thickness (ft)	92
Xf(ft)	392.7, 200
re(ft)	2000, 500

Table 4-1 Input of 64 numerical case study

4.1 Numerical cases

Firstly, the transition times determined by the product of q_{gsc} and G_p and the filling back procedure for all 64 synthetic reservoirs are compared with the actual transition times calculated inversely.

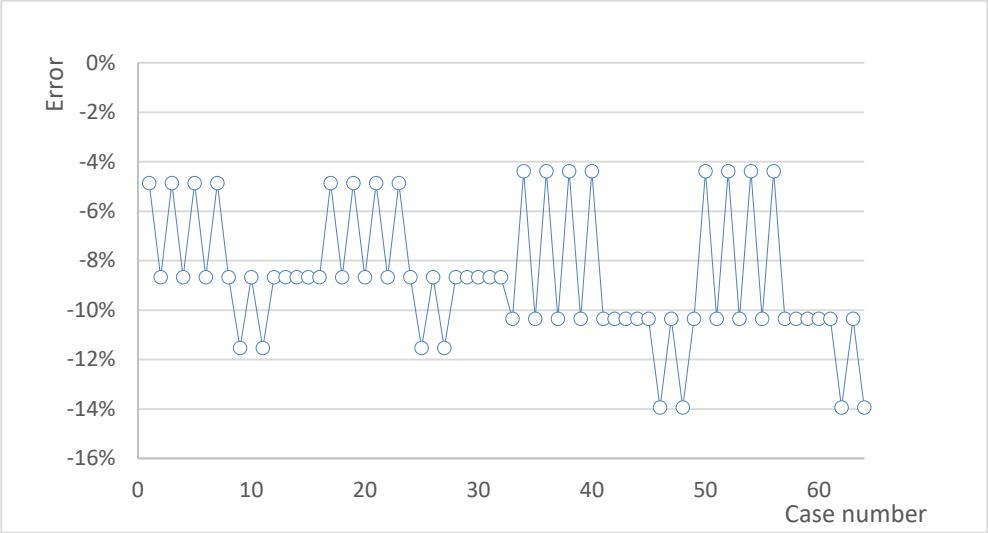

Figure 4-1 Error of determination of $\boldsymbol{t_e}$using the product of $\boldsymbol{q_{gsc}}$ and $\boldsymbol{G_p}$

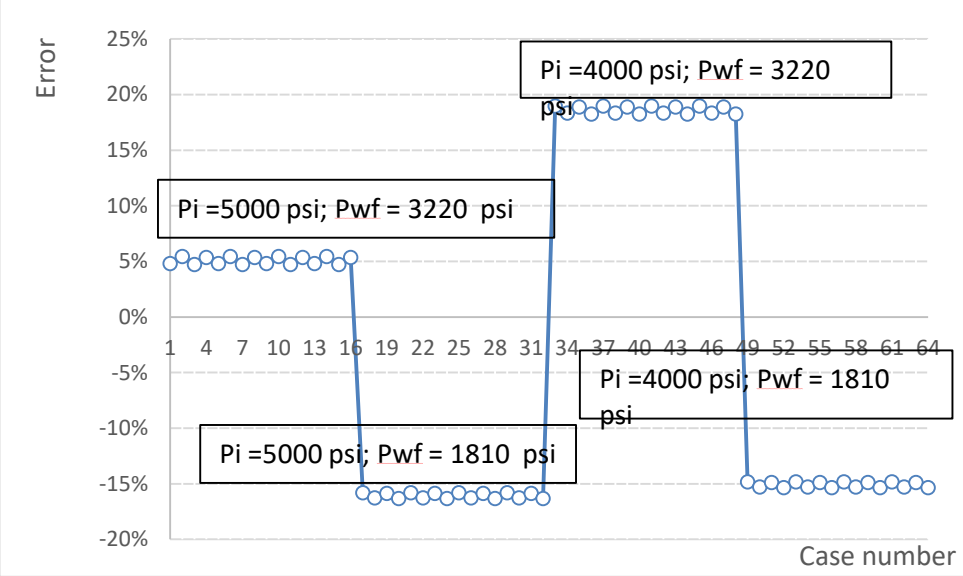

Figure 4-2 Error of determination of $\boldsymbol{t_e}$using analogous filling-back procedure

As shown in Figure 4-1, the error associated with t_e determination technique based on the product of q_{gsc} and G_p ranges between -4.87% and -13.94%,

which shows great advantage over the traditional end of half slope method. As shown in Figure 4-2, the error associated with the corresponding analogous filling-back procedure ranges between -15.87% and 18.97%. The original filling-back procedure is developed for water imbibition. The big errors of filling-back procedure results from the nonlinearities of gas flow system.

The error associated with the PDA method proposed to determine the characterization ratio $Y\sqrt{X}$ is shown in Figure 4-3. Note that this density-based PDA method is very accurate; the errors corresponding to all the 64 cases is less than 3% and ranging from -0.17% and 2.78%.

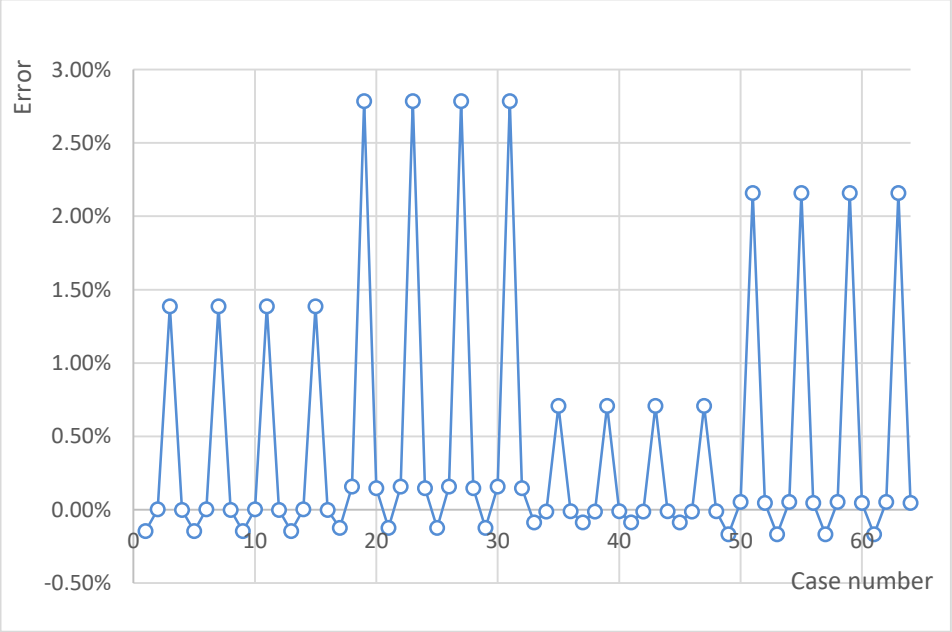

Figure 4-3 Error of PDA of determination of $\boldsymbol{Y\sqrt{X}}$

OGIP estimation is of great importance in BDF prediction. The error of OGIP estimation is associated with t_e and $Y\sqrt{X}$ determination. The errors associated with OGIP estimation is shown in Figure 4-4. As expected, the accuracy of OGIP determination based on the analogous filling-back procedure depends essentially on

the pressure arising from changing gas properties while using the product of q_{gsc} and G_p; the error associated with OGIP is generally underestimated within a small range.

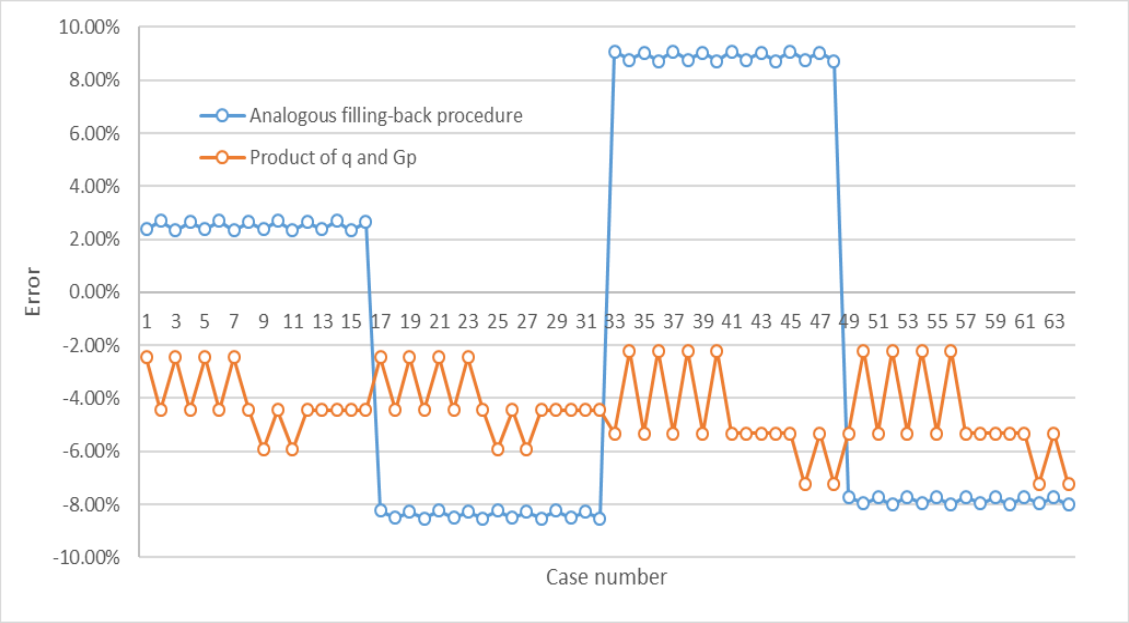

Figure 4-4 Errors of OGIP Estimation

By the determined t_e, $Y\sqrt{X}$, together with OGIP calculated, BDF prediction could be made. Figure 4-5 and Figure 4-6 shows a sample study using input shown in Table 3-1. Error analysis begins at the BDF window and ends when flow rate is less than economic flow rate, which is set as 1% of the initial gas flow rate. As we could notice, the predicted gas flow rate has very small error with numerically generated production data, and the errors keep accumulating over time. Different methods of determining t_e are tested in this example study. The biggest errors occur at the end of the production, which is less than 10% using both analogous filling-back procedure and the product of q_{gsc} and G_p. This indicates with good estimations of t_e and $Y\sqrt{X}$, the proposed BDF prediction generated relatively reliable results. However, while

using the traditional end of half slope method, the BDF prediction yields huge errors due to using inaccurate t_e values.

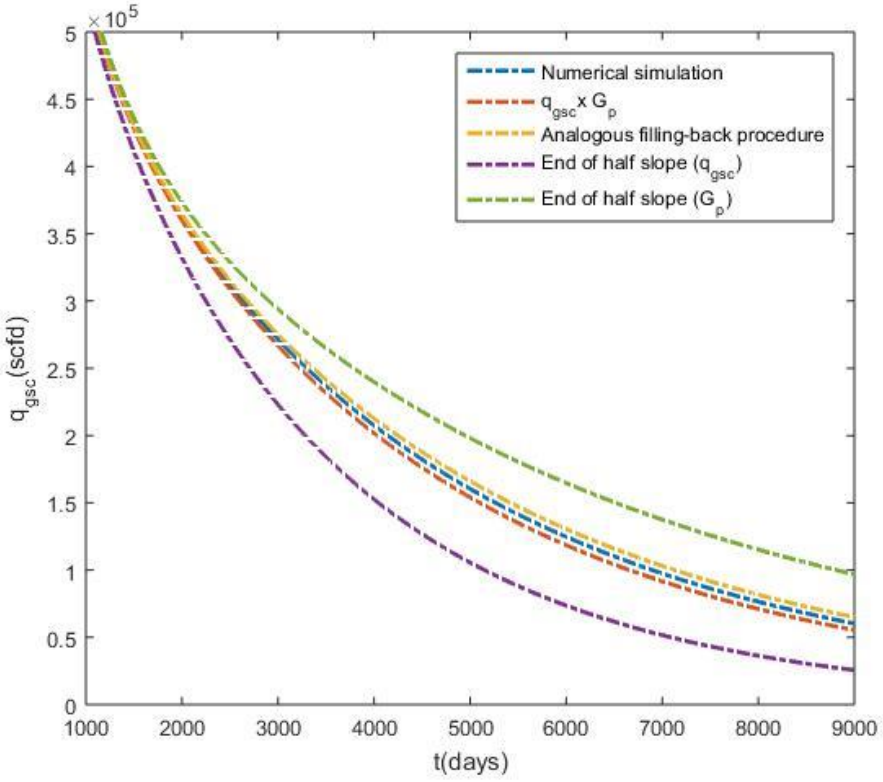

Figure 4-5 BDF prediction of the example study (Flow rate)

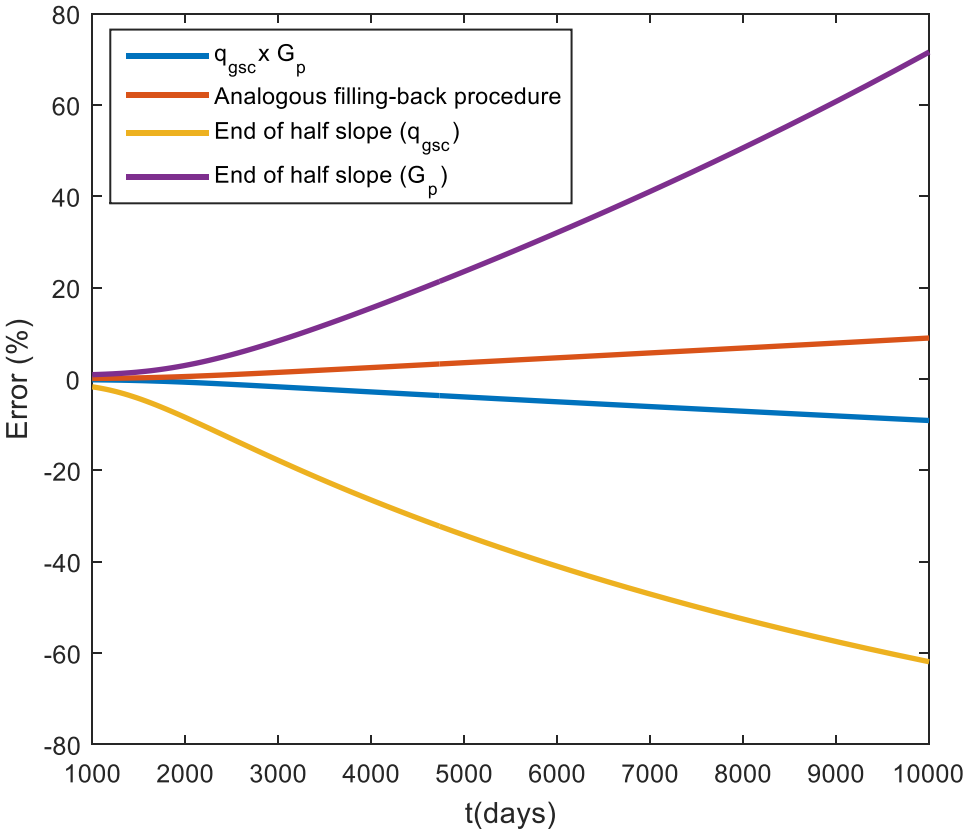

Figure 4-6 Error of BDF prediction of a sample study

It is worth noting that the predicted gas flow rate has very small error with numerically generated production data, and the errors keep accumulating over time. The small error follows from the good estimates of t_e and $Y\sqrt{X}$ that the proposed BDF prediction has generated relatively more reliable results. However, while using traditional end of half slope method, huge errors are introduced due to the inaccurate t_e determination. Mean square errors through the production life for all 64 cases are shown in Figure 4-8. It could be noticed that in overall using the product of q_{gsc} and G_p makes a better prediction through in several cases using filling back procedure generates a lower error.

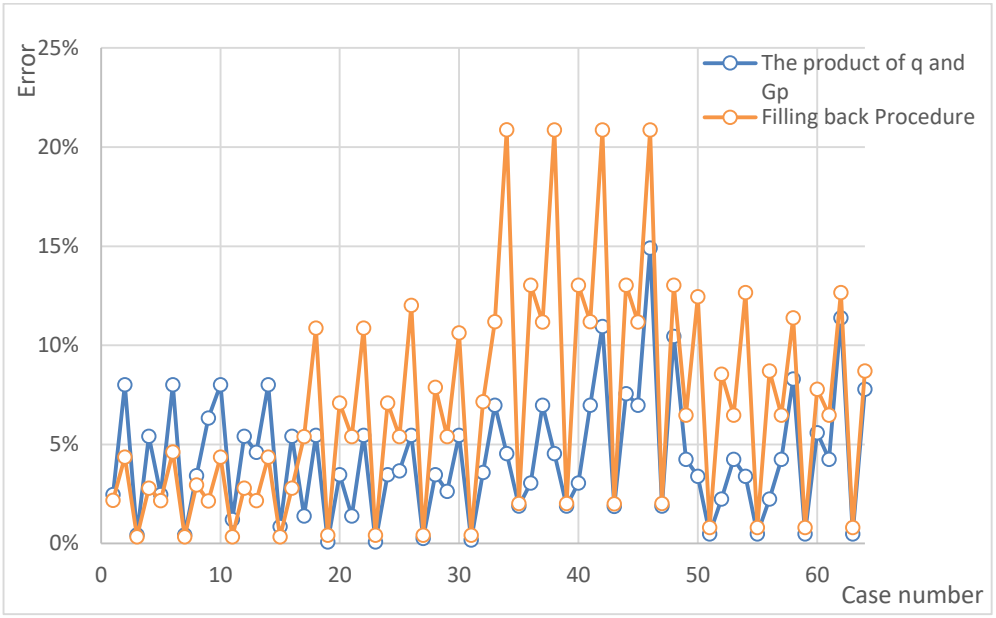

Figure 4-7 Mean squared errors of BDF Prediction of 64 Numerical Cases

4.1.1. Detailed Analysis of Synthetic Case Studies

Numerical Case A

Production data are generated using numerical simulator for analysis purpose as shown in Figure 4-8. From the plot, t_e is found to be around 5000 days easily when the product of q_{gsc} and G_p starts to deviate from the horizontal line. $Y\sqrt{X}$ is calculated to 1.187e-8 using the identified constant value 3.6e14. The analogous filling-back procedure, as shown in Figure 4-9, shows when t_D =3.3741, areas of A and B region are the same. The dimensionless time can be transformed into t_e if part of reservoir properties is known, as has been presented in section 3.2. Using the inputs value, t_e is calculated to be 4425 days. OGIP can be calculated explicitly using the obtained t_e and $Y\sqrt{X}$ values. Errors of t_e and OGIP from using end of half slope,

$q_{gsc} \cdot G_p$ method and analogous filling-back procedure are shown in Table 4-3. BDF forecasting based on the obtained t_e and $Y\sqrt{X}$ is shown in Figure 4-10.

Input	Value
Pi(psi)	5000
Pwf(psi)	1810
T (F)	290
sg	0.717
Porosity	0.15
k (md)	0.01
Thickness (ft)	92
Xf(ft)	392.7
re(ft)	2000

Table 4-2 Inputs of Numerical case

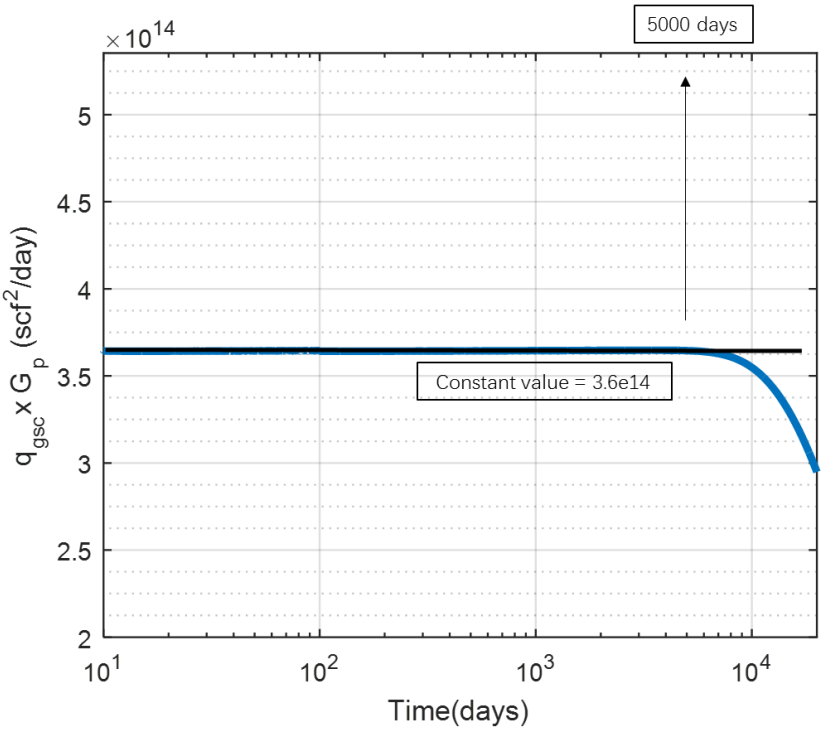

Figure 4-8 PDA - Numerical Case A

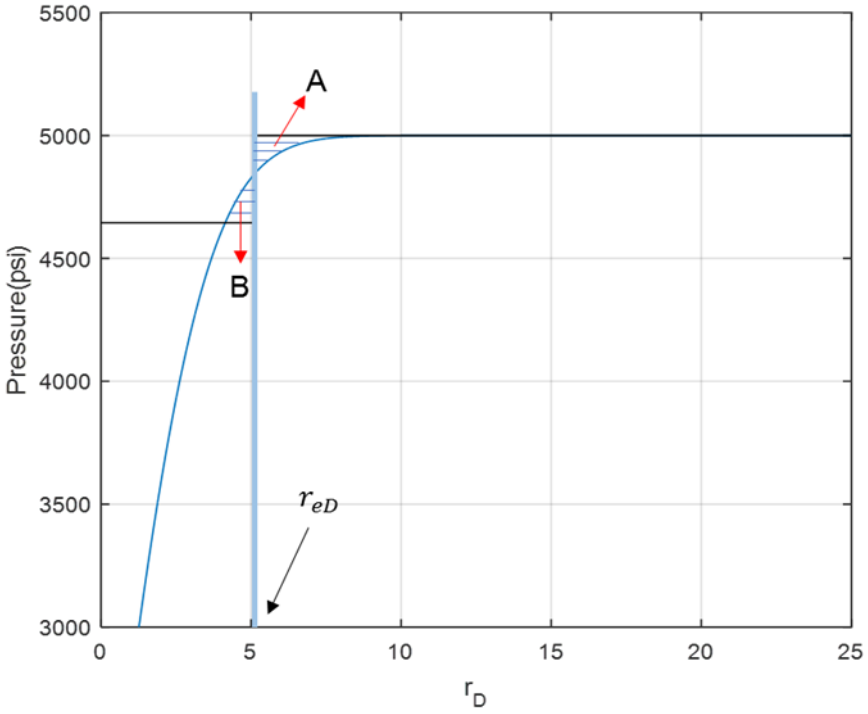

Figure 4-9 Analogous filling-back procedure - Numerical Case A

	End of half slope q_{gsc}	End of half slope G_p	Hybrid method $q_{gsc} \cdot G_p$	Analogous FB Procedure
t_e	-80.97%	90.26%	-4.87%	-15.81%
OGIP	-56.21%	38.47%	-2.09%	-7.89%

Table 4-3 Comparison of errors – Numerical Case A

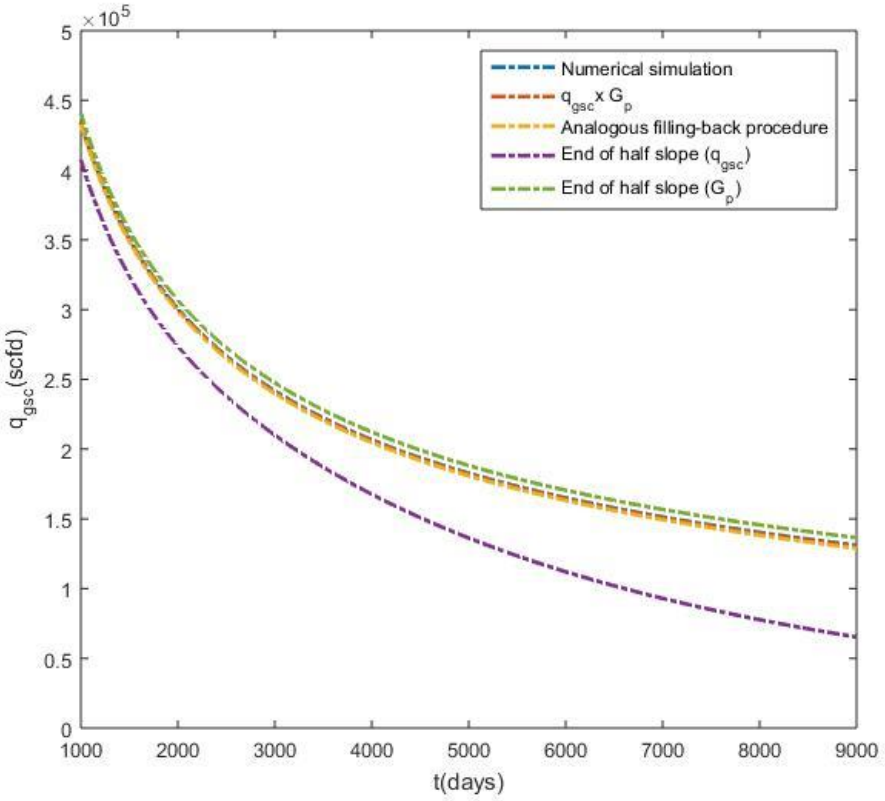

Figure 4-10 BDF gas rate prediction – Numerical Case A

Numerical Case B

Plot of $q_{gsc} \cdot G_p$ vs.t is shown in Figure 4-11 using production data generated from the numerical simulator. From the plot, t_e is found to be around 1600 days easily when the product of q_{gsc} and G_p starts to deviate from the horizontal line. $Y\sqrt{X}$ is calculated to 4.16E-8 using the identified constant value 3.15e13. The analogous filling-back procedure, as shown in Figure 4-9, shows when $t_D = 37.1075$, areas of A and B region are the same. The dimensionless time can be transformed into t_e if some reservoir properties is known, as has been presented in section 3.2. Using the inputs value, t_e is calculated to be 1474 days. Then OGIP can be calculated explicitly using the obtained t_e and $Y\sqrt{X}$ values. Errors of t_e and OGIP from using

end of half slope, $q_{gsc} \cdot G_p$ method and analogous filling-back procedure are shown in Table 4-5. BDF forecasting based on the obtained t_e and $Y\sqrt{X}$ is shown in Figure 4-13.

Input	Value
Pi(psi)	5000
Pwf(psi)	1810
T (F)	290
sg	0.717
Porosity	0.05
k (md)	0.01
Thickness (ft)	92
Xf(ft)	200
re(ft)	2000

Table 4-4 Inputs of Numerical Case B

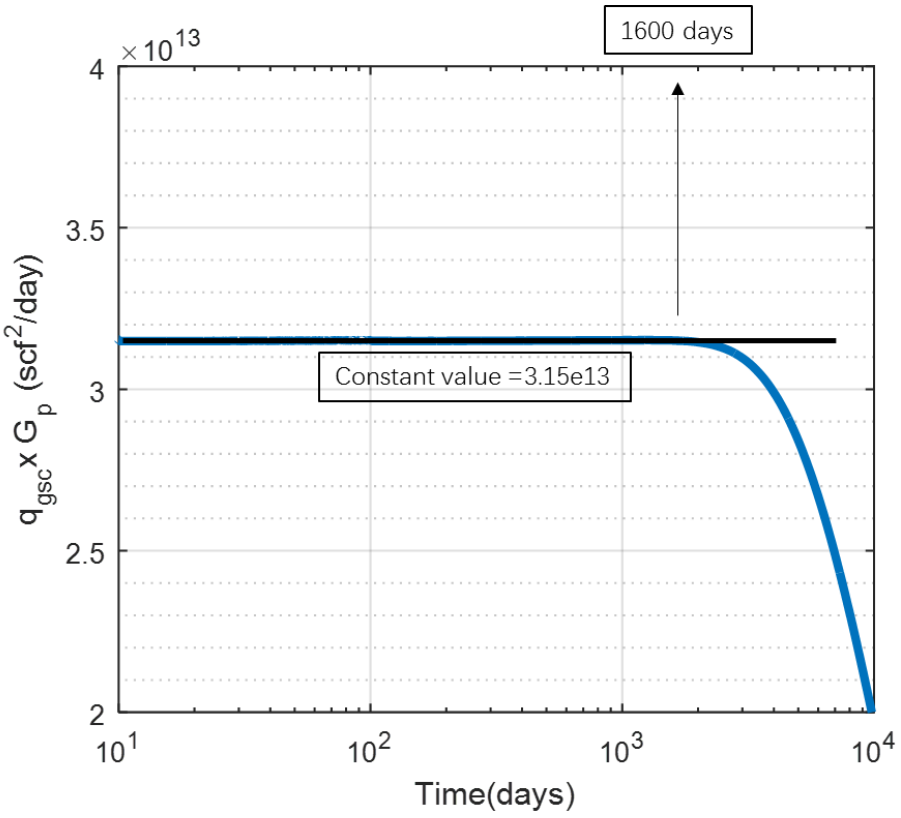

Figure 4-11 PDA - Numerical Case B

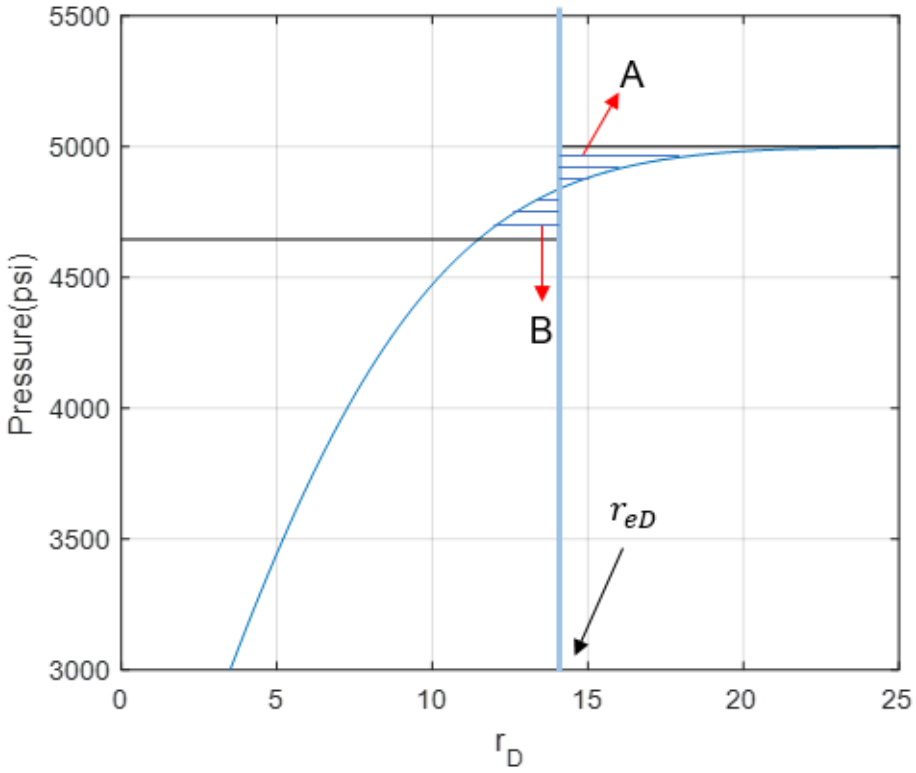

Figure 4-12 Analogous filling-back procedure - Numerical Case B

	End of half slope q_{gsc}	End of half slope G_p	Hybrid method $q_{gsc} \cdot G_p$	Analogous FB Procedure
t_e	-31.51%	185.39%	-8.68%	-15.87%
OGIP	-19.48%	64.36%	-7.03%	-10.76%

Table 4-5 Comparison of errors – Numerical Case B

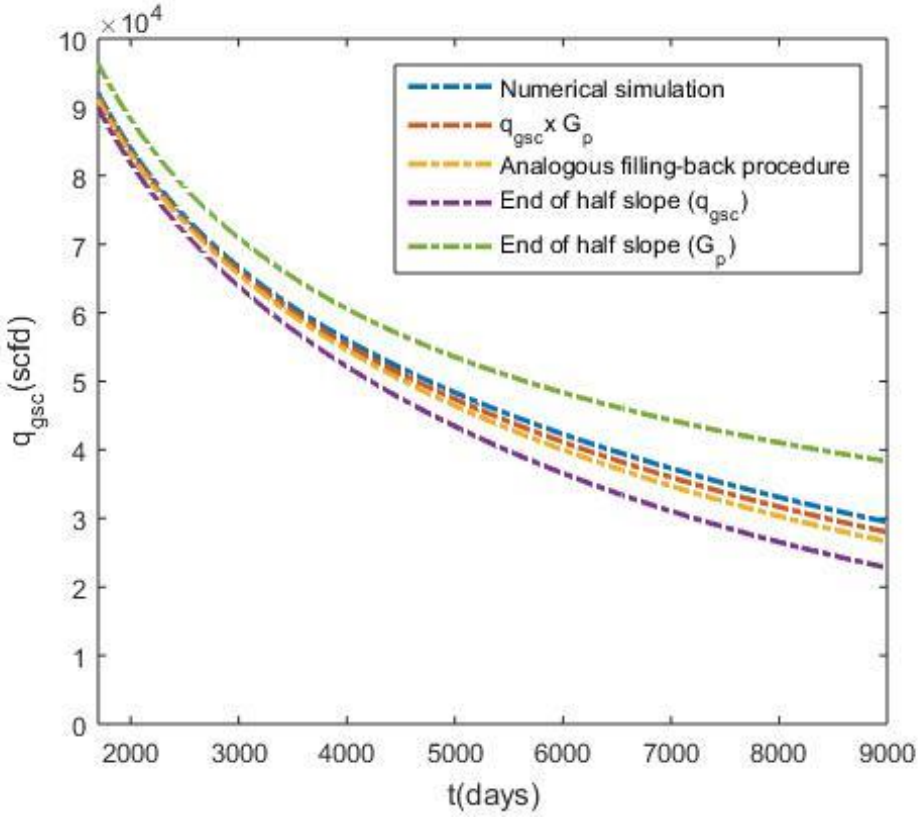

Figure 4-13 BDF gas rate prediction – Numerical Case B

As expected, BDF predictions of these two synthetic cases has small error compared to Numerical simulation, which are from the good estimates of t_e and $Y\sqrt{X}$. The traditional end of half slope method is not recommended.

4.2 Field Cases

Coapa A well

Coapa A Well is a dry gas well in a tight gas reservoir completed in Eoceno Wilcox Formation; as reported by Arevalo et al. (2001,2005). This well exhibits linear flow behavior because of the existence of natural fractures and has been producing for over 44 years with G_p= 13.527Bscf. The reported initial pressure of the reservoir is 5463 psia, with an average reservoir temperature of 230°F and specific gas gravity of 0.568. Initial water saturation is reported as 0.12. It was assumed that bottomhole pressure remains constant throughout the production. Though the P_{wf} has not been reported, it could be calculated to be 1000 psia by inversely matching the log-log diagnostic plot in the original manuscript ($\frac{\Delta m(p)}{q_{gsc}}$ vs. t). Also, occasional shut-ins exist in this production but we don't have any data available for those shut-in periods.

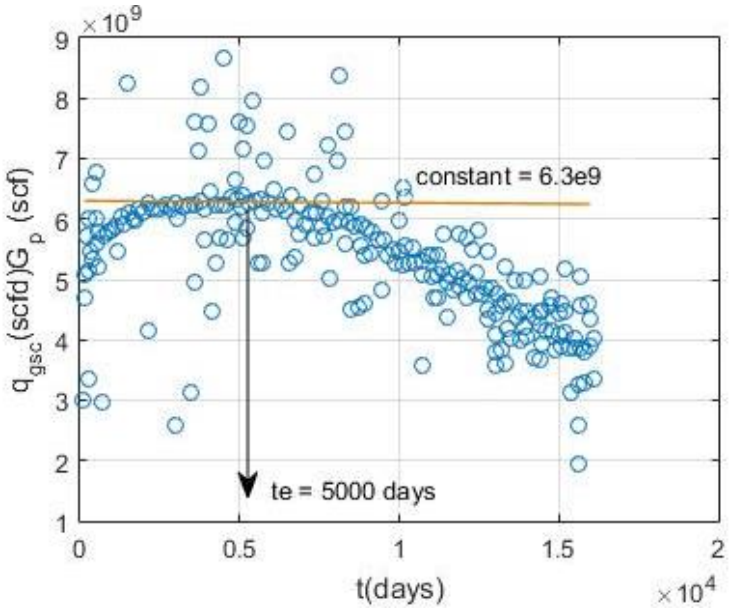

Figure 4-14 Analysis of Coapa Well A

In their study, the transition time was determined to be 6610 days; based on the time when plot of $\frac{\Delta m(p)}{q_{gsc}}$ vs. t starts bending up from straight line. Our proposed method indicates a t_e value of 5000 days as shown in Figure 4-14. The $Y\sqrt{X}$ ratio is calculated to be 3.62E-9. Using the proposed methodology, the prediction of gas production of Coapa A Well is shown in Figure 4-15 with a comparison against field data. As could be noticed, there is a little discrepancy between the BDF prediction and actual field data. Limitations of the BDF prediction are discussed later and calibrations could be made to get a better production match.

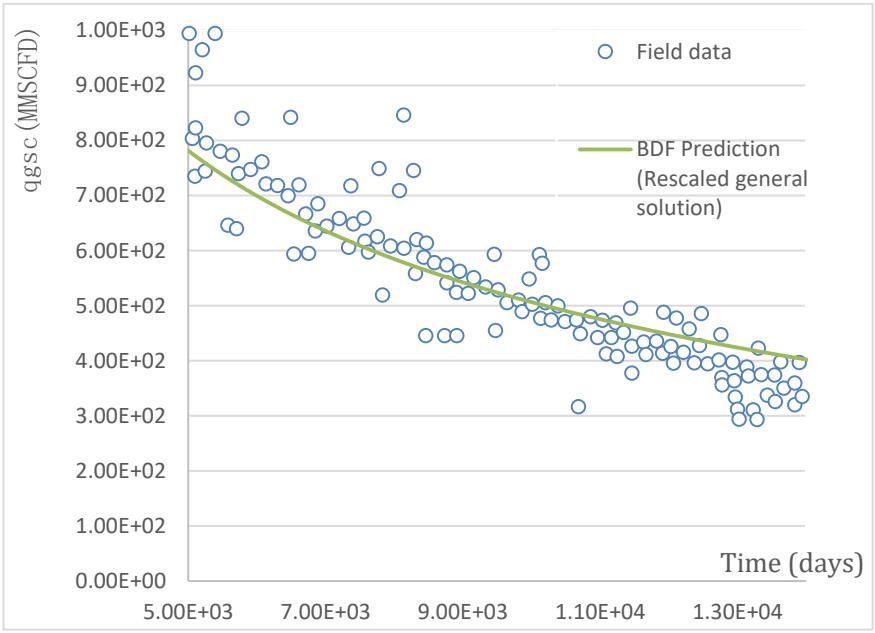

Figure 4-15 BDF Prediction of Coapa Well A (BDF window)

Dakota Well A

Dakota Well A is a tight gas well completed in San Juan basin in New Mexico and reported in Chen and Teufel (2000). This well exhibits linear flow and it has been producing gas for over 28 years with G_p= 0.55 *Bscf.* The reported initial

pressure of the reservoir is 1625 psia, with an average reservoir temperature of 125°F and specific gas gravity 0.74. Initial water saturation is reported as 0.4. The constant bottom-hole pressure of 550 psia has been used by Chen and Teufel (2000). Extreme fluctuations are found in the field data, which indicates the constant bottomhole pressure assumption may not hold.

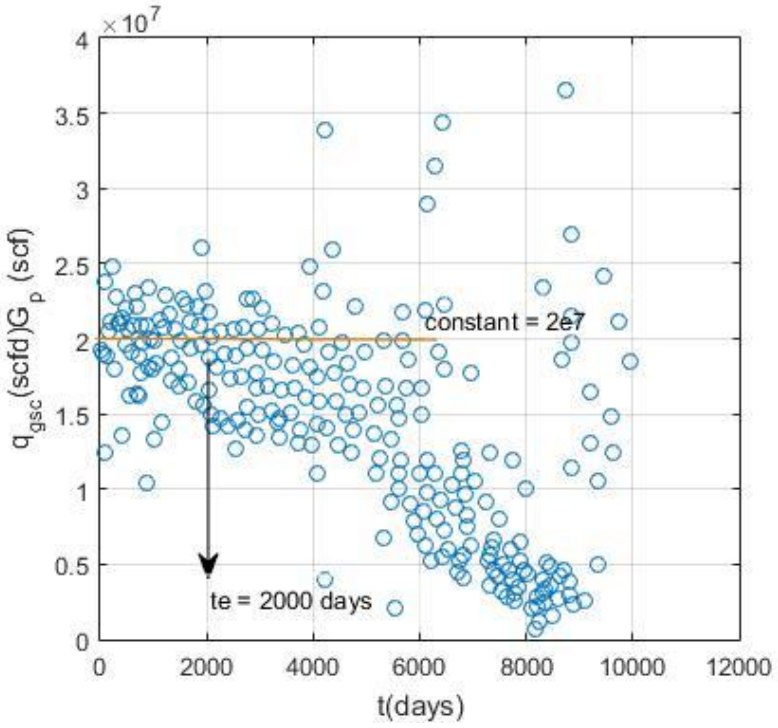

Figure 4-16 Analysis of Dakota Well A

Using the plot of the product of q_{gsc} and G_p vs. t (see Figure 4-13), the transition time has been estimated to be 2000 days. The constant value of the product is 2E7. The $Y\sqrt{X}$ ratio is calculated to be 9.31E-8. The prediction of gas production rates of Coapa A Well is shown in Figure 4-17 with a comparison against field data. The BDF prediction has an overall acceptable match with the field production data. The BDF prediction could be improved by calibrating input of the proposed BDF model as shown in the next section.

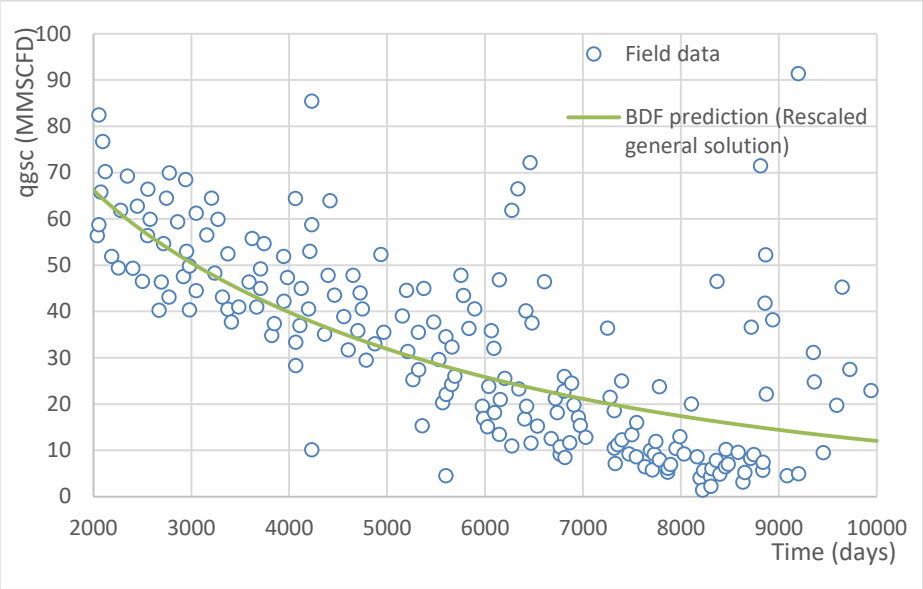

Figure 4-17 BDF Prediction of Dakota Well A (BDF window)

Calibration of prediction

The error of the predictions for field cases are as result of two reasons: 1. There are noises in the field data, which is due to occasional shut-in periods, make it harder to identify t_e and the constant product from the plot 2. The unreported shut-ins period results in overestimating reservoir size and OGIP. 3. Assumption of constant P_{wf}, which may not be true.

Many sets of reservoir simulations are conducted to see when a good history match can be obtained. Results show that by reducing reservoir size we able to get a better match with field data (Table 4-6 and Figure 4-19 Coapa A well; Table 4-7 and Figure 4-21 Dakota Well A). This indicates the primary limitation of the proposed model in the field cases is the wrong estimation of reservoir size. As mentioned, unreported occasional shut-in periods will cause overestimation of r_e. Also, numerical

simulations suggest the Cr value used (2.554) is a little high in both cases, which will cause overestimation of r_e as well.

Original		After calibration	
te	5200 days	te	4500 days

Table 4-6 Calibration of model of Coapa A well

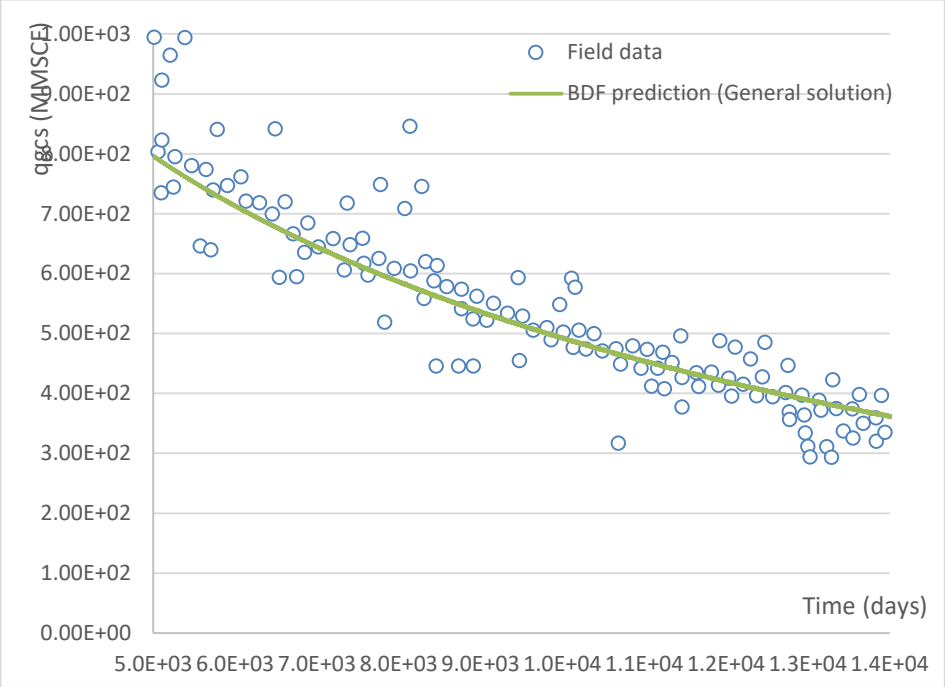

Figure 4-18 BDF prediction of Coapa A well (after calibration)

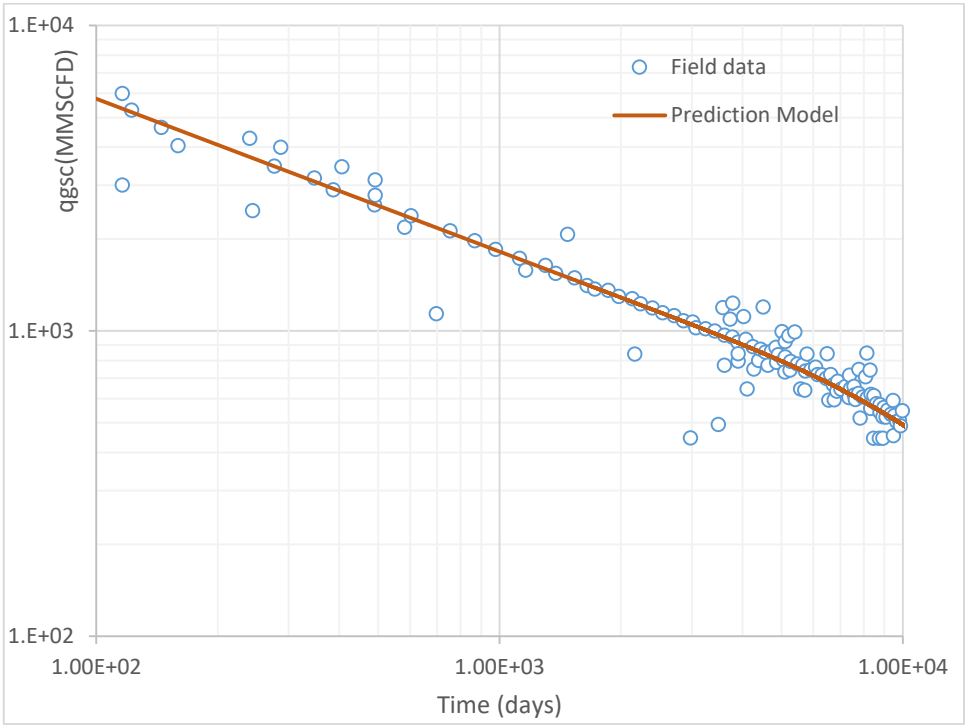

Figure 4-19 Production Prediction of Coapa A well (after calibration)

Original		After calibration	
te	2000 days	te	1600 days

Table 4-7 Calibration of model of Dakota well A

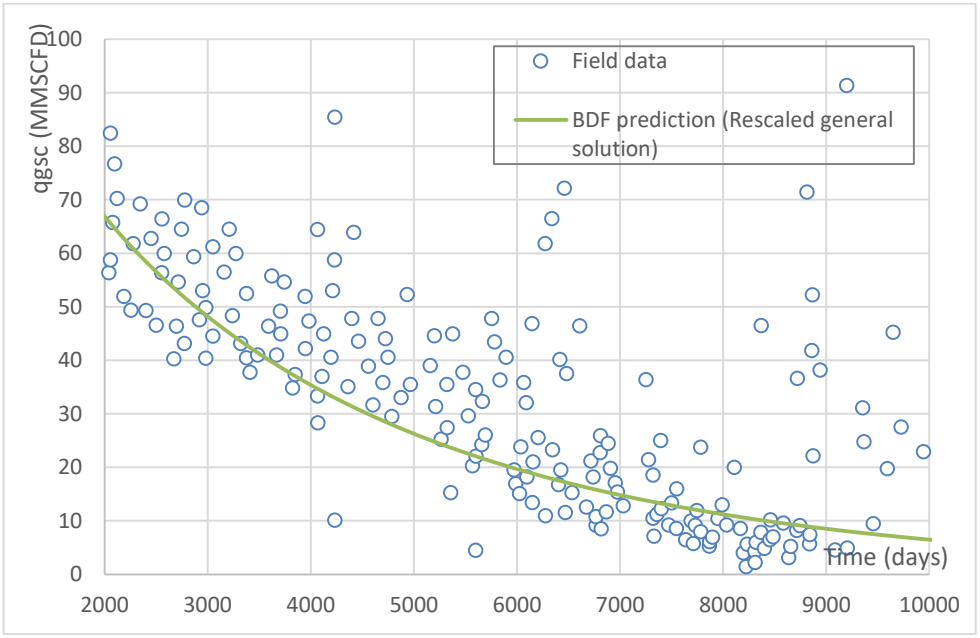

Figure 4-20 BDF prediction of Coapa A well (after calibration)

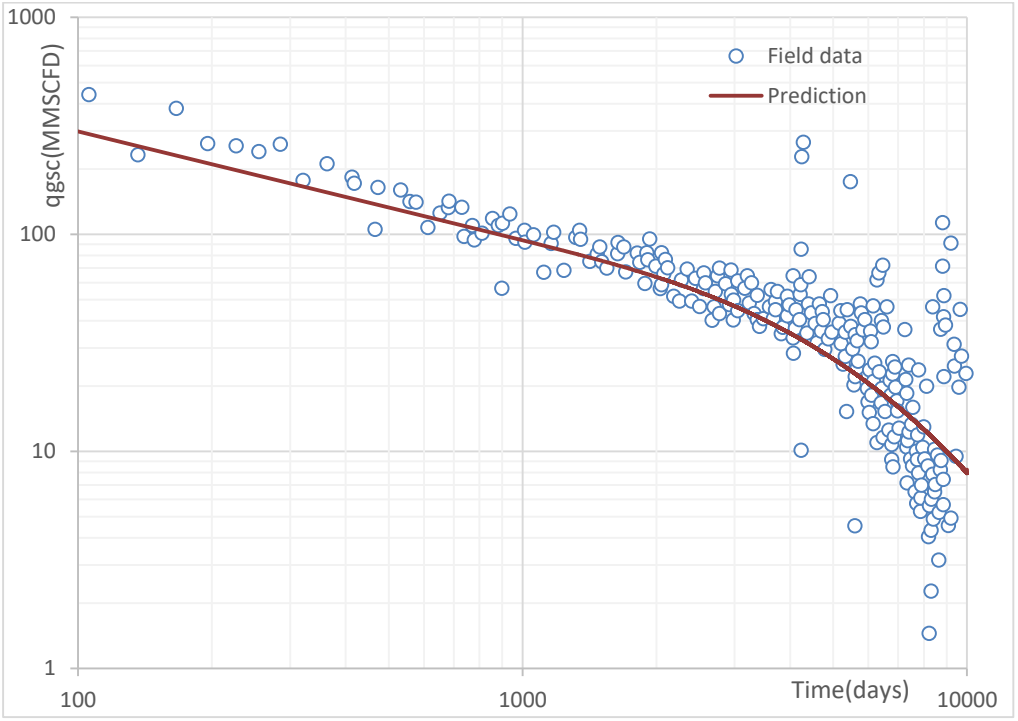

Figure 4-21 Prediction of Coapa A well (after calibration)

CHAPTER 5 - Conclusion and Summary

Based on the obtained results, the following concluding remarks can be made:

1. The proposed approach using the product of q_{gsc} and G_P could improve the accuracy by partially cancelling out errors from end of half slope method thus resulting in much better estimates of t_e. The estimated errors for the 64 numerical case studies range from 4.87% to 13.94%. Also, this approach has allowed us to conduct the analysis on a Cartesian plot, which makes it easier to spot the transition time.

2. The accuracy of these t_e determination techniques largely depends on the pressure values (reservoir pressure and bottomhole pressure). This is because the original filling-back procedure was developed for water imbibition and water properties do not vary much with change of pressure. However, in dry gas production case, changing gas properties result in nonlinearities which render the analogous filling-back procedure less accurate than the original water imbibition case. However, compared to the traditional end of half slope method, the analogous filling-back procedure could generate relatively good results. Although it requires prior knowledge of many reservoir properties—ϕ, r_e, k, X_f, we don't need any production data. Hence the method could be used to determine a priori transition time before the production if some reservoir properties are known.

3. The proposed PDA has been able to estimate the characteristic value $Y\sqrt{X}$ very accurately with an extremely small error in all the numerical cases. The accuracy of the proposed BDF model is largely based on the accuracy of t_e (reservoir size

estimation). The error of flowrate is very small at the beginning of BDF window and accumulates over time. The mean squared error for all the 64 numerical cases ranges between 4% and 19%, depending on the accuracy of t_e determination.

4. The mismatch in the field cases result from overestimation of reservoir size, which could be caused by shut-in periods and an inaccurate Cr value used.

References

Abou-Kassem, J. H., Mattar, L., & Dranchuk, P. M. (1990). Computer Calculations Of Compressibility Of Natural Gas. *Journal of Canadian Petroleum Technology*, *29*(5). https://doi.org/10.2118/90-05-10

Agarwal, R. G. (1979). "Real Gas Pseudo-Time" - A New Function For Pressure Buildup Analysis Of MHF Gas Wells. In *SPE Annual Technical Conference and Exhibition*. Society of Petroleum Engineers. https://doi.org/10.2118/8279-MS

Al-Hussainy, R., Ramey, H. J., & Crawford, P. B. (1966). The Flow of Real Gases Through Porous Media. *Journal of Petroleum Technology*, *18*(5), 624–636. https://doi.org/10.2118/1243-A-PA

Anderson, D. M., & Mattar, L. (2007). An Improved Pseudo-Time for Gas Reservoirs With Significant Transient Flow, *46*(7).

Arevalo-Villagran, J. A., Wattenbarger, R. A., Samaniego-Verduzco, F., & Pham, T. T. (2001). Production Analysis of Long-Term Linear Flow in Tight Gas Reservoirs: Case Histories. In *SPE Annual Technical Conference and Exhibition*. Society of Petroleum Engineers. https://doi.org/10.2118/71516-MS

Arevalo Villagran, J. A., Gutierrez Acosta, T., & Martinez Romero, N. (2005). Analysis of Long-Term Behavior in Tight Gas Reservoirs: Case Histories. In *SPE Latin American and Caribbean Petroleum Engineering Conference*. Society of Petroleum Engineers. https://doi.org/10.2118/95117-MS

Arps, J. J. (1945, December 1). Analysis of Decline Curves. *Society of Petroleum Engineers*. doi:10.2118/945228-G

Ayala, L., & Zhang, M. (2013). Rescaled Exponential and Density-Based Decline Models: Extension toVariable Rate/Pressure-Drawdown Conditions. *Journal of Canadian Petroleum Technology*, *52*(6), 433–440. https://doi.org/10.2118/168223-PA

Carslaw, H.S. and Jaeger, J.C. (1959). Conduction of heat in solids. *Oxford: Clarendon Press*

Chen, C., & Raghavan, R. (2013a). On the Liquid-Flow Analog To Evaluate Gas Wells Producing in Shales. *SPE Reservoir Evaluation & Engineering*, *16*(2), 209–215. https://doi.org/10.2118/165580-PA

Chen, C., & Raghavan, R. (2013b). On the Liquid-Flow Analog To Evaluate Gas Wells Producing in Shales. *SPE Reservoir Evaluation & Engineering*, *16*(2), 209–215. https://doi.org/10.2118/165580-PA

Chen, H.-Y., & Teufel, L. W. (2000). A New Rate-Time Type Curve for Analysis of Tight-Gas Linear and Radial Flows. In *SPE Annual Technical Conference and Exhibition*. Society of Petroleum Engineers. https://doi.org/10.2118/63094-MS

Clarkson, C. R. (2013a). Production data analysis of unconventional gas wells: Review of theory and best practices. *International Journal of Coal Geology*, *109*, 101–146. https://doi.org/10.1016/j.coal.2013.01.002

Clarkson, C. R. (2013b). *Production data analysis of unconventional gas wells: Workflow*. *International Journal of Coal Geology* (Vol. 109). https://doi.org/10.1016/j.coal.2012.11.016

Dranchuk, P. M., & Abou-Kassem, H. (1975). Calculation of Z Factors For Natural Gases Using Equations of State. *Journal of Canadian Petroleum Technology*, *14*(3). https://doi.org/10.2118/75-03-03

Fetkovich, M. J. (1980). Decline Curve Analysis Using Type Curves. *Journal of Petroleum Technology*, *32*(6), 1065–1077. https://doi.org/10.2118/4629-PA

Fraim, M. L. (1987). Gas Reservoir Decline-Curve Analysis Using Type Curves With Real Gas Pseudopressure and Normalized Time. *SPE Formation Evaluation*, *2*(4), 671–682. https://doi.org/10.2118/14238-PA

Ibrahim, M., & Wattenbarger, R. A. (n.d.). Rate Dependence of Transient Linear Flow in Tight Gas Wells. *Journal of Canadian Petroleum Technology*.

Kuchuk, F. J. (2009). Radius of Investigation for Reserve Estimation From Pressure Transient Well Tests. In *SPE Middle East Oil and Gas Show and Conference*. Society of Petroleum Engineers. https://doi.org/10.2118/120515-MS

Lee, A. L., Gonzalez, M. H., & Eakin, B. E. (1966). The Viscosity of Natural Gases. *Journal of Petroleum Technology*, *18*(8), 997–1000. https://doi.org/10.2118/1340-PA

Miller, F.G. (1962). Theory of unsteady-state influx of water in linear reservoirs. *Institute of Petroleum – Journal 48*(467): 365-379.

March, R., Doster, F., & Geiger, S. (2016). Accurate early-time and late-time modeling of countercurrent spontaneous imbibition. *Water Resources Research*, *52*(8), 6263–6276. https://doi.org/10.1002/2015WR018456

Mattar, L., & Anderson, D. M. (2003). A Systematic and Comprehensive Methodology for Advanced Analysis of Production Data. In *SPE Annual Technical Conference and Exhibition*. Society of Petroleum Engineers. https://doi.org/10.2118/84472-MS

Nobakht, M., & Clarkson, C. R. (2012). A New Analytical Method for Analyzing Linear Flow in Tight/Shale Gas Reservoirs: Constant-Flowing-Pressure

Boundary Condition. *SPE Reservoir Evaluation & Engineering*, *15*(3), 370–384. https://doi.org/10.2118/143989-PA

Palacio, J. C., & Blasingame, T. A. (1993). UNAVAILABLE - Decline-Curve Analysis With Type Curves - Analysis of Gas Well Production Data. In *Low Permeability Reservoirs Symposium*. Society of Petroleum Engineers. https://doi.org/10.2118/25909-MS

Qanbari, F., & Clarkson, C. R. (2013a). A new method for production data analysis of tight and shale gas reservoirs during transient linear flow period. *Journal of Natural Gas Science and Engineering*, *14*, 55–65. https://doi.org/10.1016/j.jngse.2013.05.005

Qanbari, F., & Clarkson, C. R. (2013b). A new method for production data analysis of tight and shale gas reservoirs during transient linear flow period. *Journal of Natural Gas Science and Engineering*, *14*, 55–65. https://doi.org/10.1016/j.jngse.2013.05.005

Qanbari, F., & Clarkson, C. R. (2014a). Production Data Analysis of Multi-Fractured Horizontal Wells Producing from Tight Oil Reservoirs - Bounded Stimulated Reservoir Volume. In *SPE/EAGE European Unconventional Resources Conference and Exhibition*. Society of Petroleum Engineers. https://doi.org/10.2118/167727-MS

Qanbari, F., & Clarkson, C. R. (2014b). Production Data Analysis of Multi-Fractured Horizontal Wells Producing from Tight Oil Reservoirs - Bounded Stimulated Reservoir Volume. In *SPE/EAGE European Unconventional Resources Conference and Exhibition*. Society of Petroleum Engineers. https://doi.org/10.2118/167727-MS

Van Everdingen, A. F., & Hurst, W. (1949). The Application of the Laplace Transformation to Flow Problems in Reservoirs. *Journal of Petroleum Technology*, *1*(12), 305–324. https://doi.org/10.2118/949305-G

Van Kruysdijk, C.P.J.W. and Dullaert, G.M. (1989). A Boundary Element Solution of the Transient Pressure Response of Multiple Fractured Horizontal Wells. In *2nd European Conference on the Mathematics of Oil Recovery*, Cambridge, England.

U.S. Energy Information Administration (2017, January 5). Annual Energy Outlook 2017 with projection to 2050, http://www.eia.gov/outlooks/aeo/pdf/0383(2017).pdf

Vardcharragosad, P. (2014). *LONG-TERM WELL PERFORMANCE PREDICTION IN UNCONVENTIONAL TIGHT GAS AND SHALE GAS RESERVOIRS: A DENSITY APPROACH*. (Unpublished doctoral dissertation). Pennsylvania State University, Pennsylvania, United States.

Wattenbarger, R. A., El-Banbi, A. H., Villegas, M. E., & Maggard, J. B. (2013). Production Analysis of Linear Flow Into Fractured Tight Gas Wells. In *SPE Rocky Mountain Regional/Low-Permeability Reservoirs Symposium* (pp. 265–276). Society of Petroleum Engineers. https://doi.org/10.2118/39931-MS

Ye, P., & Ayala H., L. F. (2012). A density-diffusivity approach for the unsteady state analysis of natural gas reservoirs. *Journal of Natural Gas Science and Engineering*, *7*, 22–34. https://doi.org/10.1016/j.jngse.2012.03.004

Appendix A Input of numerical studies

Case #	P_i (psi)	P_{wf} (psi)	T (F)	s_g	ϕ	k (md)	h(ft)	x_f (ft)	r_e (ft)
1	5000	3220	290	0.717	0.15	0.05	92	392.7	2000
2	5000	3220	290	0.717	0.15	0.05	92	392.7	500
3	5000	3220	290	0.717	0.15	0.05	92	200	2000
4	5000	3220	290	0.717	0.15	0.05	92	200	500
5	5000	3220	290	0.717	0.15	0.01	92	392.7	2000
6	5000	3220	290	0.717	0.15	0.01	92	392.7	500
7	5000	3220	290	0.717	0.15	0.01	92	200	2000
8	5000	3220	290	0.717	0.15	0.01	92	200	500
9	5000	3220	290	0.717	0.05	0.05	92	392.7	2000
10	5000	3220	290	0.717	0.05	0.05	92	392.7	500
11	5000	3220	290	0.717	0.05	0.05	92	200	2000
12	5000	3220	290	0.717	0.05	0.05	92	200	500
13	5000	3220	290	0.717	0.05	0.01	92	392.7	2000
14	5000	3220	290	0.717	0.05	0.01	92	392.7	500
15	5000	3220	290	0.717	0.05	0.01	92	200	2000
16	5000	3220	290	0.717	0.05	0.01	92	200	500
17	5000	1810	290	0.717	0.15	0.05	92	392.7	2000
18	5000	1810	290	0.717	0.15	0.05	92	392.7	500
19	5000	1810	290	0.717	0.15	0.05	92	200	2000
20	5000	1810	290	0.717	0.15	0.05	92	200	500
21	5000	1810	290	0.717	0.15	0.01	92	392.7	2000
22	5000	1810	290	0.717	0.15	0.01	92	392.7	500
23	5000	1810	290	0.717	0.15	0.01	92	200	2000
24	5000	1810	290	0.717	0.15	0.01	92	200	500
25	5000	1810	290	0.717	0.05	0.05	92	392.7	2000
26	5000	1810	290	0.717	0.05	0.05	92	392.7	500
27	5000	1810	290	0.717	0.05	0.05	92	200	2000
28	5000	1810	290	0.717	0.05	0.05	92	200	500
29	5000	1810	290	0.717	0.05	0.01	92	392.7	2000
30	5000	1810	290	0.717	0.05	0.01	92	392.7	500
31	5000	1810	290	0.717	0.05	0.01	92	200	2000
32	5000	1810	290	0.717	0.05	0.01	92	200	500
33	4000	3220	290	0.717	0.15	0.05	92	392.7	2000
34	4000	3220	290	0.717	0.15	0.05	92	392.7	500
35	4000	3220	290	0.717	0.15	0.05	92	200	2000
36	4000	3220	290	0.717	0.15	0.05	92	200	500
37	4000	3220	290	0.717	0.15	0.01	92	392.7	2000
38	4000	3220	290	0.717	0.15	0.01	92	392.7	500
39	4000	3220	290	0.717	0.15	0.01	92	200	2000
40	4000	3220	290	0.717	0.15	0.01	92	200	500

41	4000	3220	290	0.717	0.05	0.05	92	392.7	2000
42	4000	3220	290	0.717	0.05	0.05	92	392.7	500
43	4000	3220	290	0.717	0.05	0.05	92	200	2000
44	4000	3220	290	0.717	0.05	0.05	92	200	500
45	4000	3220	290	0.717	0.05	0.01	92	392.7	2000
46	4000	3220	290	0.717	0.05	0.01	92	392.7	500
47	4000	3220	290	0.717	0.05	0.01	92	200	2000
48	4000	3220	290	0.717	0.05	0.01	92	200	500
49	4000	1810	290	0.717	0.15	0.05	92	392.7	2000
50	4000	1810	290	0.717	0.15	0.05	92	392.7	500
51	4000	1810	290	0.717	0.15	0.05	92	200	2000
52	4000	1810	290	0.717	0.15	0.05	92	200	500
53	4000	1810	290	0.717	0.15	0.01	92	392.7	2000
54	4000	1810	290	0.717	0.15	0.01	92	392.7	500
55	4000	1810	290	0.717	0.15	0.01	92	200	2000
56	4000	1810	290	0.717	0.15	0.01	92	200	500
57	4000	1810	290	0.717	0.05	0.05	92	392.7	2000
58	4000	1810	290	0.717	0.05	0.05	92	392.7	500
59	4000	1810	290	0.717	0.05	0.05	92	200	2000
60	4000	1810	290	0.717	0.05	0.05	92	200	500
61	4000	1810	290	0.717	0.05	0.01	92	392.7	2000
62	4000	1810	290	0.717	0.05	0.01	92	392.7	500
63	4000	1810	290	0.717	0.05	0.01	92	200	2000
64	4000	1810	290	0.717	0.05	0.01	92	200	500

Appendix B Derivation of BDF Prediction (LTA with MB adjustment)

As discussed in Section 2.4, the LTA solution with material balance adjustment provides the most accurate results.

The rescaled LTA solution for gas is expressed as:

$$q_{Dd}{}^{*gas,LTA} = \bar{\lambda} \cdot \exp\left(-\bar{\beta} t_{DAd}{}^{*}\right) \quad \text{Equation B-1}$$

Replacing the dimensionless decline flow rate and the decline time by the real flow rate and time values,

$$\frac{\pi r_{eD}}{4} Y \frac{q_{gsc}}{r_p} = \bar{\lambda} \cdot exp\left(-\frac{\pi^2}{4 r_{eD}^2} X \bar{\beta} t\right) \quad \text{Equation B-2}$$

Using the definition of region of influence,

$$r_{eD} = C_r \cdot \left(\frac{\alpha_1 k t_e x_f^2}{\phi \mu_{gi} C_{gi}}\right)^{0.5} \quad \text{Equation B-3}$$

From Equation 2-4 and Equation 2-5 we get the expressions for X and Y:

$$X = \frac{\alpha_1 k}{\phi \mu_{gi} c_{gi} x_f^2} \quad \text{Equation B-4}$$

$$Y = \frac{\mu_{gi} c_{gi} \rho_{sc}}{2\pi \alpha_1 k h \rho_i} \quad \text{Equation B-5}$$

Substituting X, Y and r_{eD} into Equation 0-12:

$$q_{gsc} = \bar{\lambda}\, r_\rho \frac{4}{\pi} \frac{1}{C_r \sqrt{t_e}} \frac{1}{Y\sqrt{X}} exp\left(-\frac{\pi^2}{4} \frac{1}{C_r^2 t_e} \bar{\beta} t\right) \quad \text{Equation B-6}$$

As noted in Section 2-4, in order to get accurate $\bar{\lambda}$ and $\bar{\beta}$ value, material balance adjustment is desired to do long-time approximation solution. The rescaled *material balance solution* for gas is expressed as:

$$q_{Dd}{}^{*gas,LTA} = \bar{\lambda} \cdot \frac{3}{2}\, exp\left(-\frac{12}{\pi^2}\bar{\beta} t_{DAd}{}^{*}\right) \qquad \text{Equation B-7}$$

Replacing the dimensionless decline flow rate and the decline time by the real flow rate and time values:

$$\frac{\pi r_{eD}}{4} Y \frac{q_{gsc}}{r_p} = \bar{\lambda} \cdot \frac{3}{2} \cdot exp\left(-\frac{12}{\pi^2}\frac{\pi^2}{4r_{eD}^2} X\bar{\beta} t\right) \qquad \text{Equation B-8}$$

Substituting X, Y and r_{eD} into Equation 0-8, we have

$$q_{gsc} = \bar{\lambda}\, r_p \frac{6}{\pi}\ \frac{1}{C_r\sqrt{t_e}}\ \frac{1}{Y\sqrt{X}}\ exp\left(-\frac{3}{C_r^2 t_e}\bar{\beta} t\right) \qquad \text{Equation B-9}$$

Appendix C Derivation of OGIP estimation

In this ideal linear flow system where fractures extend to the reservoir boundaries, as depicted in Figure 2-1, OGIP is calculated as:

$$OGIP = \frac{4x_f h\phi r_e}{B_{gi}} \quad \text{Equation C-1}$$

OGIP could be expressed as a function of $Y\sqrt{X}$ and t_e. Using the expression for r_e and $Y\sqrt{X}$ is calculated using the definition of Y and X:

$$r_e = C_r \cdot \left(\frac{\alpha_1 k t_e}{\phi \mu_{gi} c_{gi}}\right)^{0.5} \quad \text{Equation C-2}$$

$$\frac{1}{Y\sqrt{X}} = \left(2\pi\sqrt{\alpha_1}\frac{\rho_i}{\rho_{sc}}\frac{h\sqrt{\phi}}{\sqrt{\mu_{gi}C_{gi}}}\right) \quad \text{Equation C-3}$$

The product of Equation 0-4 and Equation 0-11 is:

$$\frac{\sqrt{t_e}}{Y\sqrt{X}} = \left(\frac{2\pi}{C_r}\frac{\rho_i}{\rho_{sc}}\right) X_f h\phi r_e = \frac{2\pi}{C_r}\cdot\frac{x_f h\phi r_e}{B_{gi}} \quad \text{Equation C-5}$$

Hence, OGIP can be expressed as:

$$OGIP = \frac{4X_f h\phi r_e}{B_{gi}} = \frac{4\sqrt{t_e}}{Y\sqrt{X}} \Big/ \left(\frac{2\pi}{C_r}\right) \quad \text{Equation C-6}$$

Appendix D Procedure of BDF Prediction

At time step 1, $\bar{\lambda}$ is calculated at initial reservoir condition and $\bar{\beta}^{<1>}$ = 1:

$$\bar{\lambda}^{<1>} = \frac{\mu_{gi} c_{gi}}{2\theta\left(\frac{\bar{\rho} - \rho_{wf}}{\bar{\psi} - \psi_{wf}}\right)} \qquad \text{Equation D-1}$$

And gas flow rate at time step 1 gas rate is calculated as:

$$q_{gsc}^{<1>} = \bar{\lambda}^{<1>} r_\rho \frac{4}{\pi} \frac{1}{C_r \sqrt{t_e}} \frac{1}{Y\sqrt{X}} \sum_{n_{odd}}^{\infty} exp\left(-\frac{\pi^2}{4} \frac{1}{C_r^2 t_e} \bar{\beta}^{<1>} t^{<1>}\right)$$

Equation D-2

Cumulative production at time step 1 is calculated as:

$$\mathrm{G_p}^{<1>} = q_{gsc}^{<1>} * t^{<1>} \qquad \text{Equation D-3}$$

Average reservoir density at time step 2 is calculated from material balance statement using Cumulative production at time step 1:

$$\frac{\bar{\rho}^{<2>}}{\rho_i} = \left(1 - \frac{G_p^{<1>}}{OGIP}\right) \qquad \text{Equation D-4}$$

$\bar{\lambda}$ is calculated again as:

$$\bar{\lambda}^{<2>} = \frac{\mu_{gi} c_{gi}}{2\theta\left(\frac{\bar{\rho}^{<2>} - \rho_{wf}}{\bar{\psi} - \psi_{wf}}\right)} \qquad \text{Equation D-5}$$

$\bar{\beta}$ is calculated as:

$$\bar{\beta}^{<2>} = \frac{1}{t^{<2>}} \int_0^{t^{<2>}} \bar{\lambda}\, dt$$

Equation D-6

Flow rate at time step 2:

$$q_{gsc}^{<2>} = \bar{\lambda}^{<2>}\, r_\rho \frac{4}{\pi}\, \frac{1}{C_r\sqrt{t_e}}\, \frac{1}{Y\sqrt{X}} \sum_{n_{odd}}^{\infty} exp\left(-\frac{\pi^2}{4}\frac{1}{C_r^2 t_e}\bar{\beta}^{<2>} t^{<2>}\right)$$

Equation D-7

For all the following time step, continue the calculation as:

$$\frac{\bar{\rho}^{<i+1>}}{\rho_i} = (1 - \frac{G_p^{<i>}}{OGIP})$$

Equation D-8

$$\bar{\lambda}^{<i+1>} = \frac{\mu_{gi} c_{gi}}{2\theta(\frac{\bar{\rho}^{<2>} - \rho_{wf}}{\bar{\psi} - \psi_{wf}})}$$

Equation D-9

$$\bar{\beta}^{<i+1>} = \frac{1}{t^{<i+1>}} \int_0^{t^{<i+1>}} \bar{\lambda}\, dt$$

$$q_{gsc}^{<i+1>}$$

$$= \bar{\lambda}^{<i+1>}\, r_\rho \frac{4}{\pi}\, \frac{1}{C_r\sqrt{t_e}}\, \frac{1}{Y\sqrt{X}} \sum_{n_{odd}}^{\infty} exp\left(-\frac{\pi^2}{4}\frac{1}{C_r^2 t_e}\bar{\beta}^{<i+1>} t^{<i+1>}\right)$$

Equation D-10